

The Pennsylvania State University
The Graduate School
College of Engineering

**THE EFFECT OF SPECIFIC IONS ON THE PERMSELECTIVITY OF ION
EXCHANGE MEMBRANES**

A Thesis in
Chemical Engineering
by
Harrison J. Cassady

© 2016 Harrison J. Cassady

Submitted in Partial Fulfillment
of the Requirements
for the Degree of

Master of Science

August 2016

The thesis of Harrison J. Cassady was reviewed and approved* by the following:

Michael A. Hickner
Associate Professor of Materials Science and Engineering
Thesis Co-Advisor

Manish Kumar
Assistant Professor of Chemical Engineering
Thesis Co-Advisor

Bruce E. Logan
Kappe Professor of Environmental Engineering

Phillip E. Savage
Department Head of Chemical Engineering

*Signatures are on file in the Graduate School.

Abstract

Ion exchange membranes are a class of selective barriers that prevent the passage of some aqueous ions (co-ions), while allowing other ions (counter-ions) to pass unimpeded. Ion exchange membranes form a critical component in many clean energy and ionic separation applications, and can be used to generate electricity, store and convert energy, desalinate sea water and treat highly toxic mine waste. In the effort to slow global warming, new clean energy technologies are needed to replace traditional fossil fuel sources. The improvement of ion exchange membranes will allow technologies based on these barriers to become more economical, and will provide new tools to fight climate change.

Water uptake and permselectivity were measured for five sulfonated poly(ether sulfone) cation exchange membranes with varying degrees of functionalization from 20 % to 60 %. Tests were conducted in aqueous salt solutions of LiCl, NaCl, KCl, Li₂SO₄, Na₂SO₄ and K₂SO₄, to isolate the effect of counter-ions and co-ions on membrane permselectivity. Water uptake ranged from 0.13 g_{water}/g_{polymer} to 0.76 g_{water}/g_{polymer} depending on the degree of functionalization and salt used, but was not found to describe the permselectivity differences between salts as the counter-ion and co-ion were varied. This lack of correlation between water uptake and permselectivity is counter to some previous reports. Counter-ion

binding affinity, charge density and dilute solution mobility were identified as factors influencing membrane permselectivity. Specifically, counter-ions with higher binding affinities to the fixed charge group of the polymer showed lower permselectivities due to counter-ion condensation. Co-ion polarizability was identified as the primary factor for co-ion effects on permselectivity, with more polarizable co-ions resulting in lower membrane permselectivities.

Table of Contents

List of Figures	vii
List of Tables	viii
Acknowledgments	ix
Chapter 1	
Ion exchange polymers and their use in permselective membranes	1
References	5
Chapter 2	
A review of past research on ion exchange membranes	10
2.1 Basic theory of ion exchange membranes	10
2.2 Membrane resistance	11
2.2.1 Individual contribution of boundary layers to resistance .	16
2.2.2 Transport numbers	17
2.3 Membrane permselectivity	19
2.4 Specific ion effects	20
2.4.1 Bi-ionic membrane potential	21
2.4.2 Nanophase separation	24
2.5 Membrane upper bound theory	24
2.6 Asymmetric membranes	26
2.6.1 Surface modification	27
2.6.2 Phase inversion	27
2.6.3 Thin-film composite membranes	28
References	29
Chapter 3	
Specific Ion Effects on the Permselectivity of Sulfonated Poly(Ether Sulfone) Cation Exchange Membranes	35
3.1 Introduction	35

3.2	Materials and methods	36
3.2.1	Ion exchange membranes	36
3.2.2	Water uptake	37
3.2.3	Permselectivity	38
3.3	Results and Discussion	43
3.3.1	Water uptake	43
3.3.2	Counter-ion effects on permselectivity	46
3.3.3	Co-ion effects on permselectivity	48
3.4	Conclusions	51
	References	51
 Chapter 4		
	Conclusions and future work	54
4.1	Future work	55
4.1.1	Specific ion effects on permselectivity	55
4.1.2	Polymer property effects on permselectivity	58
	References	59

List of Figures

2.1	Chemical structure of Nafion	11
2.2	Transport of salt through an ion exchange membrane	12
2.3	Current-voltage curves for various membranes.	15
2.4	Individual components of membrane resistance for several membranes	17
2.5	Intrinsic resistance of AEMs in 0.5 mol L^{-1} sodium chloride or ammonium bicarbonate	23
2.6	SANS results for various AEMs	25
2.7	Influence of free volume element size on water and sodium chloride diffusivity and the water/salt selectivity in BPS and BPSH membranes.	26
2.8	SEM cross section images of asymmetric membranes produced by phase inversion	28
3.1	Chemical structure of sulfonated poly(ether sulfone)	37
3.2	Cell for measuring membrane potential for a membrane subject to a concentration gradient. The electrodes are placed 1 cm from the membrane surface and the membrane area is 10 cm^2	44
3.3	Permselectivity versus water uptake for SPES cation exchange membranes in various salts	45
3.4	Permselectivity versus counter-ion binding affinity for SPES CEMs	47
3.5	Counter-ion interactions with the fixed charge group	48

List of Tables

2.1	Ionic composition of seawater.	21
3.1	Properties of the sulfonated poly(ether sulfone) polymers used in this study.	37
3.2	Mean activity coefficients used for salts at different concentrations.	42
3.3	Permselectivity for a selected membrane in various salts	46
3.4	Properties of the cations and anions considered in this study.	46
4.1	Property data for ions that are recommended for future membrane permselectivity testing.	56

Acknowledgments

The path to this degree has not been lonely. For the last three years my life has been filled with exceptional people doing marvelous things, and for this I am very lucky. I would like to thank everybody who has been in my life for these last few years; epic adventures, good discussions, theories dissected, experiments run, TV shows watched, through thick and thin, I owe my happiness and my success to you. I would also like to take a moment to give special recognition to several specific people who have played a key role during my time here.

First, I would like to thank Dr. Mike Hickner, my thesis advisor, for supporting me intellectually, financially, and for teaching me how to tweak my writing style to get the subtleties of my message just right. You were at the core of this journey, and I cannot thank you enough for being there with me along the way. I would also like to thank Dr. Geoff Geise for providing a good base for me to start from, and being a good mentor to me for the time you were here, and Dr. Manish Kumar, for helping me through some rough decisions.

I must also mention my fellow labmates: TJ Zimudzi, Doug Kushner, Clara and Junior Capparelli, Sarah and Garrett Smedley, Changwoo Nam, Liang Zhu and Sean Nuñez. Thank you all for making the day fun, for laughing, joking, speculating, criticizing and complaining. An empty office is a scary thought

indeed. I also must thank Paul Browning for providing such formidable competition during our interoffice bake offs. I would also like to thank my undergraduate research assistants, Will Salem, Emily Cimino and Victoria Christensen making my life a lot easier. You guys rocked in the lab, and I hope you all find yourself doing the things you love to do.

I would also like to extend a big thank you to Cathy Krause for all of the assistance in interfacing with the graduate school and the department. No matter how dire the situation, you were always able to work wonders to make sure everything was ready at every step of the way.

I am also grateful to the financial support that Air Products and PPG have provided me along the way. I always had the supplies I needed to do good science, and it was good to be reminded of what life in the real world is like every once in a while.

I would like to thank Kevin Shebek, Will Elliott and Becky Johnson for being killer friends.

Finally, I would like to thank family for being with me from day one (well, day 793 and 1521 for my sisters), as well as Anais Becerra and her son Imanol.

To all my friends in State College and beyond, thank you for filling my life with happiness. I can't wait to discover what's next.

Chapter 1 |

Ion exchange polymers and their use in permselective membranes

Rapid industrialization over the last two centuries has strained world energy supplies and threatens the stability of the global climate. Atmospheric carbon dioxide levels have increased by 142 % since 1750.^[1] Thermal expansion of seawater as well as arctic ice melting at a rate of 2.7 % per decade has contributed to a rise in global sea level of 1.3 mm/year for the past twenty years.^[2,3] A study examining climate-induced behavioral changes in plants and animals found 80 % of species to exhibit shifts in directions congruent with global warming.^[4] It is known with high confidence that anthropogenic emission of greenhouse gases and consequent global warming is responsible for these, as well as other changes.^[5-7] The rapid development and implementation of clean energy sources is critical to minimizing environmental, ecological and economical damages while ensuring a hospitable world for future generations.^[8-10]

Apart from geothermal and nuclear power, almost all terrestrial energy sources originate from the sun. While fossil fuels provide an enormous historical cache of the sun's energy, renewable energy strives to use the sun's energy that reaches us now. Considering that evaporation of ocean water consumes 25 % of the

solar energy that reaches the earth, this is a logical place to look for renewable energy.^[11,12] While only 10 % of evaporated seawater ever falls as precipitation over land, conversion of gravitational potential energy from this cycle in hydroelectric dams currently provides one-fifth of the world's electricity.^[13]

The salt concentration gradient formed by the evaporation of sea water to form fresh water contains an immense amount of untapped energy.^[14,15] The global potential released in concentration gradients is upwards of 1.9 TW, of which an estimated 980 GW is available for extraction.^[16,17] Reverse electrodialysis (RED) uses anion exchange membranes (AEMs) and cation exchange membranes (CEMs) to convert the entropy of mixing into usable electric energy. Just as a hydroelectric power plant is placed at locations where there exists a large potential energy gradient, a reverse electrodialysis plant can be built near large concentration gradients, such as where the Ganges River river runs into the Bay of Bengal, to provide a source of clean energy. The Ganges River discharges 38 129 m³/s of fresh water into the Bay of Bengal, releasing 2.4 TW of energy from the mixing of fresh water with salt water, roughly equivalent to our current global power consumption.^[18] Even a tiny fraction of this released power would contribute an enormous amount of electricity to the 500 million people that live in this region.^[19]

Many renewable energy technologies generate power disproportionately throughout the day; solar power does not provide power at night, and windmills are subject to the whim of the breeze. Without a way to store and redistribute this energy, a large amount of renewable energy generated will be wasted. Ion exchange membranes are found in many energy storage technologies that have the potential to capture and redistribute the energy produced via renewable means. For example, a redox flow battery uses ion exchange membranes to store

energy in external tanks of electrolyte solution for recovery later, providing an large energy storage capacity at a fraction of the cost of a traditional battery.^[20-23] PEM fuel cells use a proton exchange membrane (PEM) sandwiched between two platinum electrodes to extract the chemical potential energy released when hydrogen and oxygen gas react to form water. This allows hydrogen produced using renewable energy technologies to be used in small-scale applications such as automobiles or in remote locations.^[24-26]

Ion exchange membranes are used extensively for the separation of ionic species. Electrodialysis uses an applied electrochemical current to push ions through an alternating series of anion exchange membranes and cation exchange membranes. While currently uneconomical for concentrated saline solutions, electrodialysis is frequently used for the desalination of brackish water, and can also be used to remove toxic heavy metals from the effluent of industrial process streams.^[27-29]

Ion exchange membranes have also found use in sensors, and have been used to build sensors for carbon monoxide, hydrogen, sulfur dioxide, chlorine, ammonia and propane.^[30-32]

A critical element for the performance of technologies that rely on ion exchange membranes is the ability of the ion exchange membrane to form an effective barrier to undesirable ions, while allowing desirable ions to transport unimpeded. The improvement of membrane permselectivity and resistance is crucial for advancing the use of ion exchange membranes in energy and separation applications.

Sodium chloride is the most commonly used electrolyte for the characterization of ion exchange membranes.^[33-36] Sodium chloride is used because it is cheap, has properties that are well known, and is the most prevalent electrolyte

found in nature. While sodium chloride provides a good baseline for the simple characterization of ion exchange membranes, many of the processes for which ion exchange membranes are used involve other electrolytes, and sodium chloride is not completely representative of membrane performance in other salts. For example, ammonium bicarbonate is a thermolytic salt that can be used in a closed-loop low grade waste heat recovery system, however ion exchange membranes have been found to have lower permselectivity in ammonium bicarbonate solutions than sodium chloride solutions of the same concentration.^[37-39] Ion exchange membranes are also exposed to other salts when used in real-world systems, such as the ocean which contains a large number of dissolved ions in solution (see Table 2.1).

The current theoretical models for the transport of ions in ion exchange membranes do not account for differences in the electrolyte beyond changes in the activity coefficient for different salts. Current theory predicts that two electrolytes of equivalent solution activity will perform identically for all membranes. In practice, membrane transport properties of a given salt are not indicative of properties for other salts in the membrane.^[40-42] For a single salt system, both the counter- and co-ion are known to change the ionic transport properties within a membrane. Changes in ion valence have a particularly strong influence on transport properties, but significant changes have been shown even for ions of the same valence.^[38,43,44] While the influence of these ions on an ideal system with a perfectly permselective membrane is described theoretically,^[45] a knowledge gap exists on how different ions impact the permselectivity and ionic resistance in ion exchange membranes.

The objective of this thesis is to measure ion-specific effects on the membrane transport properties permselectivity and ionic resistance. A method for relating

membrane potential to permselectivity for divalent ions was developed, which can aid in constructing a theoretical framework to describe ion-specific effects in charged polymers. Understanding co-ion and counter-ion effects on membrane performance will ultimately be used to modify polymer properties such as charge density, water uptake, fixed-ion type, polymer structure and cross-linking density to produce custom, highly optimized ion exchange membranes for specific processes such as flow batteries, fuel cells, hydrogen production or energy conversion.

References

1. World Meteorological Organization. *Record greenhouse gas levels impact atmosphere and oceans* Press Release 1002 (Sept. 2014). URL: http://www.wmo.int/pages/mediacentre/press_releases/pr_1002_en.html.
2. Dasgupta, S., Laplante, B., Meisner, C., Wheeler, D. & Yan, J. The impact of sea level rise on developing countries: a comparative analysis. *Climatic Change* **93**, 379–388 (2008).
3. Nicholls, R. J. & Cazenave, A. Sea-level rise and its impact on coastal zones. *Science* **328**, 1517–1520 (2010).
4. Root, T. L. *et al.* Fingerprints of global warming on wild animals and plants. *Nature* **421**, 57–60 (2003).
5. Bernstein, L. *et al.* *Climate change 2007: Synthesis report. Summary for Policy-makers* tech. rep. (IPCC, Valencia, 2007).
6. Broeke, M. v. d. *et al.* Partitioning recent greenland mass loss. *Science* **326**, 984–986 (2009).
7. Colwell, R. K., Brehm, G., Cardelús, C. L., Gilman, A. C. & Longino, J. T. Global warming, elevational range shifts, and lowland biotic attrition in the wet tropics. *Science* **322**, 258–261 (2008).
8. Dresselhaus, M. S. & Thomas, I. L. Alternative energy technologies. *Nature* **414**, 332–337 (2001).
9. Herzog, A. V., Lipman, T. E. & Kammen, D. M. Renewable energy sources. *Encyclopedia of Life Support Systems Forerunner Volume*. (2001).
10. Poizot, P. & Dolhem, F. Clean energy new deal for a sustainable world: from non-CO₂ generating energy sources to greener electrochemical storage devices. *Energy & Environmental Science* **4**, 2003–2019 (2011).
11. Lindsey, R. *Climate and earth's energy budget* NASA Earth Observatory. URL: <http://earthobservatory.nasa.gov/Features/EnergyBalance> (2009).
12. Betts, A. K. *The climate energy balance of the earth* URL: <http://alanbetts.com/understanding-climate-change/question/the-climate-energy-balance-of-the-earth/> (2013).

13. Perlman, H. *The water cycle: Evaporation* USGS. URL: <http://water.usgs.gov/edu/watercycleevaporation.html> (2014).
14. Wick, G. L. Power from salinity gradients. *Energy* **3**, 95–100 (1978).
15. Lacey, R. Energy by reverse electro dialysis. *Ocean Engineering* **7**, 1–47 (1980).
16. Ramon, G. Z., Feinberg, B. J. & Hoek, E. M. V. Membrane-based production of salinity-gradient power. *Energy & Environmental Science* **4**, 4423 (2011).
17. Post, J. W. *Blue energy: electricity production from salinity gradients by reverse electro dialysis* Ph.D. (Wageningen University and Research Centre, Wageningen, Netherlands, 2009).
18. International Energy Agency. *Key World Energy Statistics 2015* tech. rep. (2015). URL: <http://www.iea.org/publications/freepublications/publication/key-world-energy-statistics-2015.html>.
19. Ganga Action Parivar. *About Ganga* URL: <http://www.gangaaction.org/about-ganga/> (2016).
20. Wang, W. *et al.* Recent Progress in Redox Flow Battery Research and Development. *Advanced Functional Materials* **23**, 970–986 (2013).
21. Li, X., Zhang, H., Mai, Z., Zhang, H. & Vankelecom, I. Ion exchange membranes for vanadium redox flow battery (VRB) applications. *Energy & Environmental Science* **4**, 1147 (2011).
22. Xi, J., Wu, Z., Qiu, X. & Chen, L. Nafion/SiO₂ hybrid membrane for vanadium redox flow battery. *Journal of Power Sources* **166**, 531–536 (2007).
23. Ponce de León, C., Frías-Ferrer, A., González-García, J., Szánto, D. A. & Walsh, F. C. Redox flow cells for energy conversion. *Journal of Power Sources* **160**, 716–732 (2006).
24. Barbir, F. *PEM Fuel Cells* in *Fuel Cell Technology* (ed MBA, P. N. S. B.) (Springer London, 2006), 27–51.
25. Zhang, J. *PEM Fuel Cell Electrocatalysts and Catalyst Layers: Fundamentals and Applications* (Springer Science & Business Media, 2008).
26. Mann, R. F. *et al.* Development and application of a generalised steady-state electrochemical model for a PEM fuel cell. *Journal of Power Sources* **86**, 173–180 (2000).
27. Pilat, B. Practice of water desalination by electro dialysis. *Desalination. Desalination and the environment water shortage* **139**, 385–392 (2001).
28. Van der Bruggen, B. & Vandecasteele, C. Distillation vs. membrane filtration: overview of process evolutions in seawater desalination. *Desalination* **143**, 207–218 (2002).

29. Wódzki, R., Sionkowski, G. & Poźniak, G. Recovery and concentration of metal ions. IV. Uphill transport of Zn(II) in a multimembrane hybrid system. *Separation Science and Technology* **34**, 627–649 (1999).
30. Otagawa, T. *et al.* Planar microelectrochemical carbon monoxide sensors. *Sensors and Actuators B: Chemical* **1**, 319–325 (1990).
31. Yasuda, A. & Shimidzu, T. Electrochemical carbon monoxide sensor with a Nafion® film. *Reactive and Functional Polymers* **41**, 235–243 (1999).
32. Knake, R., Jacquinet, P., Hodgson, A. W. E. & Hauser, P. C. Amperometric sensing in the gas-phase. *Analytica Chimica Acta* **549**, 1–9 (2005).
33. Długołęcki, P., Nymeijer, K., Metz, S. & Wessling, M. Current status of ion exchange membranes for power generation from salinity gradients. *Journal of Membrane Science* **319**, 214–222 (2008).
34. Greenlee, L. F., Lawler, D. F., Freeman, B. D., Marrot, B. & Moulin, P. Reverse osmosis desalination: Water sources, technology, and today's challenges. *Water Research* **43**, 2317–2348 (2009).
35. Tanaka, Y. Mechanism of low permeability treatment for bivalent ions through an ion exchange membrane. *Journal of the Electrochemical Society of Japan* **42**, 26 (1974).
36. Tanaka, Y. & Senō, M. Treatment of ion exchange membranes to decrease divalent ion permeability. *Journal of Membrane Science* **8**, 115–127 (1981).
37. Logan, B. E. & Elimelech, M. Membrane-based processes for sustainable power generation using water. *Nature* **488**, 313–319 (2012).
38. Geise, G. M., Hickner, M. A. & Logan, B. E. Ammonium bicarbonate transport in anion exchange membranes for salinity gradient energy. *ACS Macro Letters* **2**, 814–817 (2013).
39. Geise, G. M., Cassady, H. J., Paul, D. R., Logan, B. E. & Hickner, M. A. Specific ion effects on membrane potential and the permselectivity of ion exchange membranes. *Physical Chemistry Chemical Physics* **16**, 21673–21681 (2014).
40. Güler, E., van Baak, W., Saakes, M. & Nijmeijer, K. Monovalent-ion-selective membranes for reverse electrodialysis. *Journal of Membrane Science* **455**, 254–270 (2014).
41. Weber, A. Z. *et al.* Redox flow batteries: a review. *Journal of Applied Electrochemistry* **41**, 1137–1164 (2011).
42. Irvine, G. J., Rajesh, S., Georgiadis, M. & Phillip, W. A. Ion selective permeation through cellulose acetate membranes in forward osmosis. *Environmental Science & Technology* **47**, 13745–13753 (2013).

43. Geise, G. M., Hickner, M. A. & Logan, B. E. Ionic resistance and permselectivity tradeoffs in anion exchange membranes. *ACS Applied Materials & Interfaces* **5**, 10294–10301 (2013).
44. Geise, G. M., Paul, D. R. & Freeman, B. D. Fundamental water and salt transport properties of polymeric materials. *Progress in Polymer Science* **39**, 1–42 (2014).
45. Helfferich, F. G. *Ion exchange* (Dover Publications, New York, 1962).

Chapter 2 |

A review of past research on ion exchange membranes

2.1 Basic theory of ion exchange membranes

Ion exchange polymers are created by attaching a charged species to a polymer backbone, as shown in Figure 2.1. The degree to which the polymer has been functionalized is given by the degree of functionalization, which is the fraction of functionalized repeat units to total repeat units: $d.f. = m/(m+n)$.

As the degree of functionalization increases, the polymer becomes more hydrophobic and will begin to swell when placed in an aqueous solution. Since the functionalized ions are fixed to the polymer backbone, the concentration of functionalized ions (fixed ion concentration) and their associated mobile counter-ions set a minimum ionic concentration that can exist within the polymer. If this fixed ion concentration is greater than the ionic concentration of the solution, an entropic pressure against additional anion/cation mobile salt pairs from entering the polymer will exist. Since it is entropically unfavorable for an anion/cation mobile pair to adsorb into the polymer, the primary mobile charge carriers within the polymer are the mobile counter-ions associated with functional groups. If the fixed ion concentration is set high enough, the concentration of co-ions in the polymer becomes effectively zero, resulting in a polymer where counter-ions are

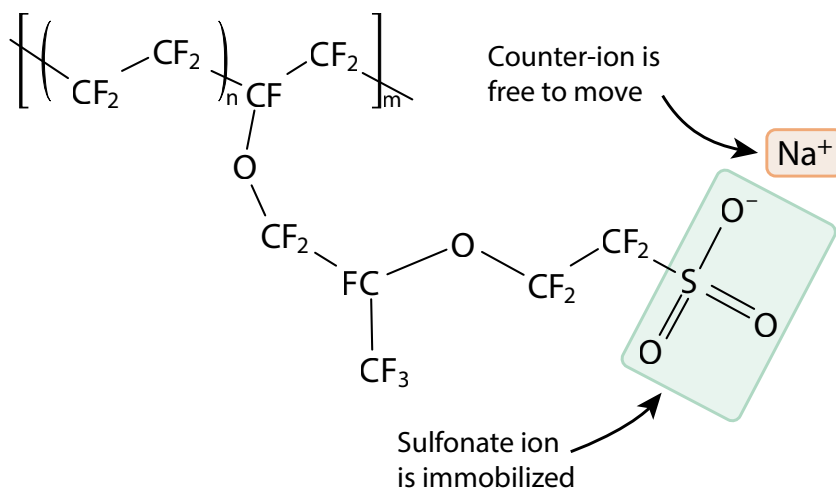


Figure 2.1: Chemical structure of Nafion. Nafion was developed by DuPont in the 1960s and is one of the most widely used cation exchange polymers in the world.

the only mobile species available for transport.

Membranes composed of ion exchange polymers are called ion exchange membranes, and are found as either anion exchange membranes (AEMs) that restrict the transport of cations, or cation exchange membranes (CEMs) that restrict the transport of anions.

2.2 Membrane resistance

The resistance of an ion exchange membrane describes how the material impedes ionic flux through the membrane. When a driving force is applied to an ion exchange membrane (e.g. electrochemical potential, concentration difference) ions will move. A membrane with a higher resistance will sustain a lower flux of ions for a given driving force than a membrane with a lower resistance. Therefore, membranes with a low resistance are desirable for nearly all applications.

The transport of ions in a solution/membrane system occurs through four distinct regions: the bulk solution region, the diffusion boundary layer, the electric

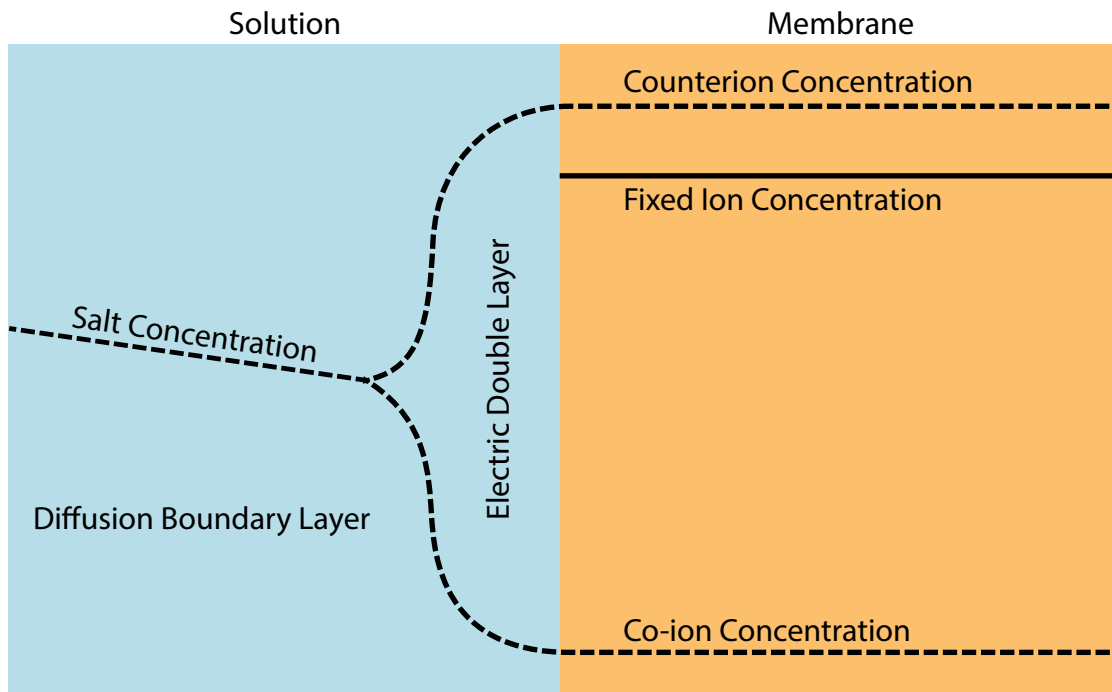


Figure 2.2: Transport of salt through an ion exchange membrane showing the three regions in which ion transport occurs.

double layer and the membrane region. Figure 2.2 shows the ionic concentration profile of an electrolyte as it transports through a membrane. Ions will transport differently through each region, so understanding the mechanisms of diffusion within each region is important.

In the bulk solution region, the equivalent concentration of co-ions and counter-ions available to carry a current are equal. In this region, the amount of current carried by the co-ion relative to the counter-ion is determined by the ratio of each ions solution mobility. For a salt where the solution mobility of each ion is nearly equivalent, such as KCl, this means half of the current is carried by the K^+ ion, and half of the solution is carried by the Cl^- ion.

In the membrane region, the large concentration of fixed charged groups sets a minimum counter-ion concentration that is greater than the salt concentration

in solution. This results in Donnan exclusion of co-ions, as indicated by the low co-ion concentration in Figure 2.2.

When the concentration of ions is different on each side of the membrane, ions will transport to equalize the concentrations. Transport cannot take place however, as the co-ions cannot transport through the membrane, resulting in a diffusion potential that balances the concentration driving force across the membrane. This diffusion potential is given by:^[1]

$$E_{\text{diff}} = \frac{RT}{F} \int_{\bar{a}'_i}^{\bar{a}''_i} \sum \frac{t_i}{z_i} d \ln a_i \quad (2.1)$$

where t_i is the transport number of ion i , z_i is the charge of ion i , a'_i is the activity of ion i at one membrane interface and a''_i is the activity of ion i at the other membrane interface.

The electric double layer occurs due to the discontinuity in ionic concentration that occurs at the interface between solution and membrane. The electric double layer breaks electroneutrality locally (it is balanced by the electric double layer on the other side of the membrane) as the ionic concentrations of counter-ions and co-ions rapidly change concentration between the solution and membrane. The potential across the electric double layer is given by the Donnan potential:

$$E_{\text{don}} = \frac{RT}{F} \ln \frac{a_i}{\bar{a}_i} \quad (2.2)$$

where a_i is the activity of ion i at the solution side of the electric double layer, and \bar{a}_i is the activity of ion i at the membrane side of the electric double layer.

Finally, the diffusion boundary layer occurs because the transport number of ions are different between the membrane and the solution. This results in an

accumulation of salt on one side of the membrane, and a depletion of salt on the other. The concentration profile of the diffusion boundary layer is given by:

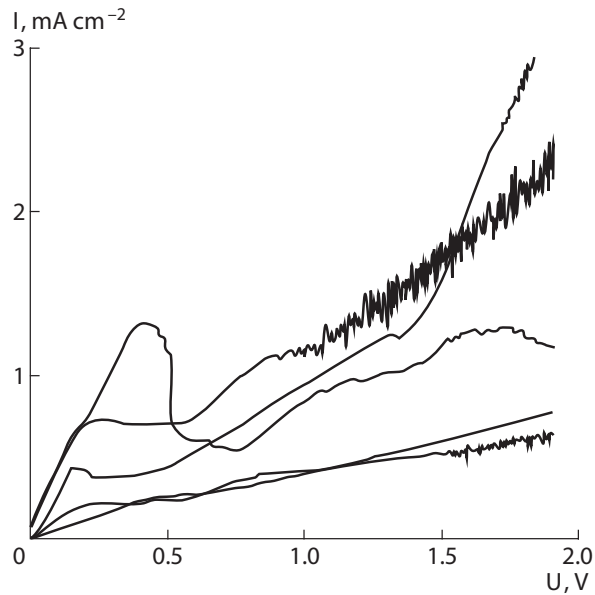
$$J_a = -D_a \frac{dC_a}{dx} \quad (2.3)$$

where J_a is the flux of salt A through the diffusion system, D_a is the diffusion coefficient of salt A, and C_a is the concentration of salt A at position x of the diffusion boundary layer.

Unlike the diffusion potential and electric double layer which are intrinsic to a given membrane and solution, the diffusion boundary layer is highly dependent on a the hydrodynamic environment of the system. Factors such as system mixing, solution flow rate and container size all affect the size of the diffusion boundary layer.

For an unmixed system the diffusion boundary layer will grow in size indefinitely, until it reaches the edge of the container. For a mixed system, the size of the diffusion boundary layer will depend on the hydrodynamic environment of the membrane, as well as the magnitude of the ion flux through the system. In general, more mixing reduces the size of the diffusion boundary layer and a higher flux increases the size of the diffusion boundary layer,^[2] however predicting the exact size of the diffusion boundary layer is difficult due to the complex nature of fluid dynamics.

Since the diffusion boundary layer can cause both an increase and decrease in salt concentration, issues relating to high and low salt concentrations can result. For example, if the concentration of salt increases to the solubility limit, precipitation can occur, fouling the membrane. Alternatively, as the salt concentration decreases, ionic resistance through the diffusion boundary layer increases. If



Rubinstein *et al.* [4]

Figure 2.3: Current-voltage curves for various membranes.

the diffusion boundary layer reaches a point where the concentration is zero, no charge carriers are left to carry a current. This point is called the limiting current, and is characterized by a sharp increase in membrane resistance.^[3]

Figure 2.3 shows a typical current-voltage plot for an ion exchange membrane.^[4] Initially the measured current increases linearly with applied voltage in what is termed the ohmic region. Eventually the current reaches the limiting current and plateaus as expected from the theory discussed above. As the voltage is increased beyond the point at which current plateaus, at some point the current begins to increase linearly again, albeit with higher amount of noise in what is termed the over-limiting current region.

The explanation for this over-limiting current has eluded researchers for years, with theories such as water electrolysis at the membrane surface, or a loss of membrane permselectivity being proposed.^[5,6] Ultimately it has been shown that small defects in the membrane result in an imperfect charge distribution at

the surface. These differences in surface charge result in an electro-convective mixing effect, disrupting the diffusion boundary layer.^[7,8]

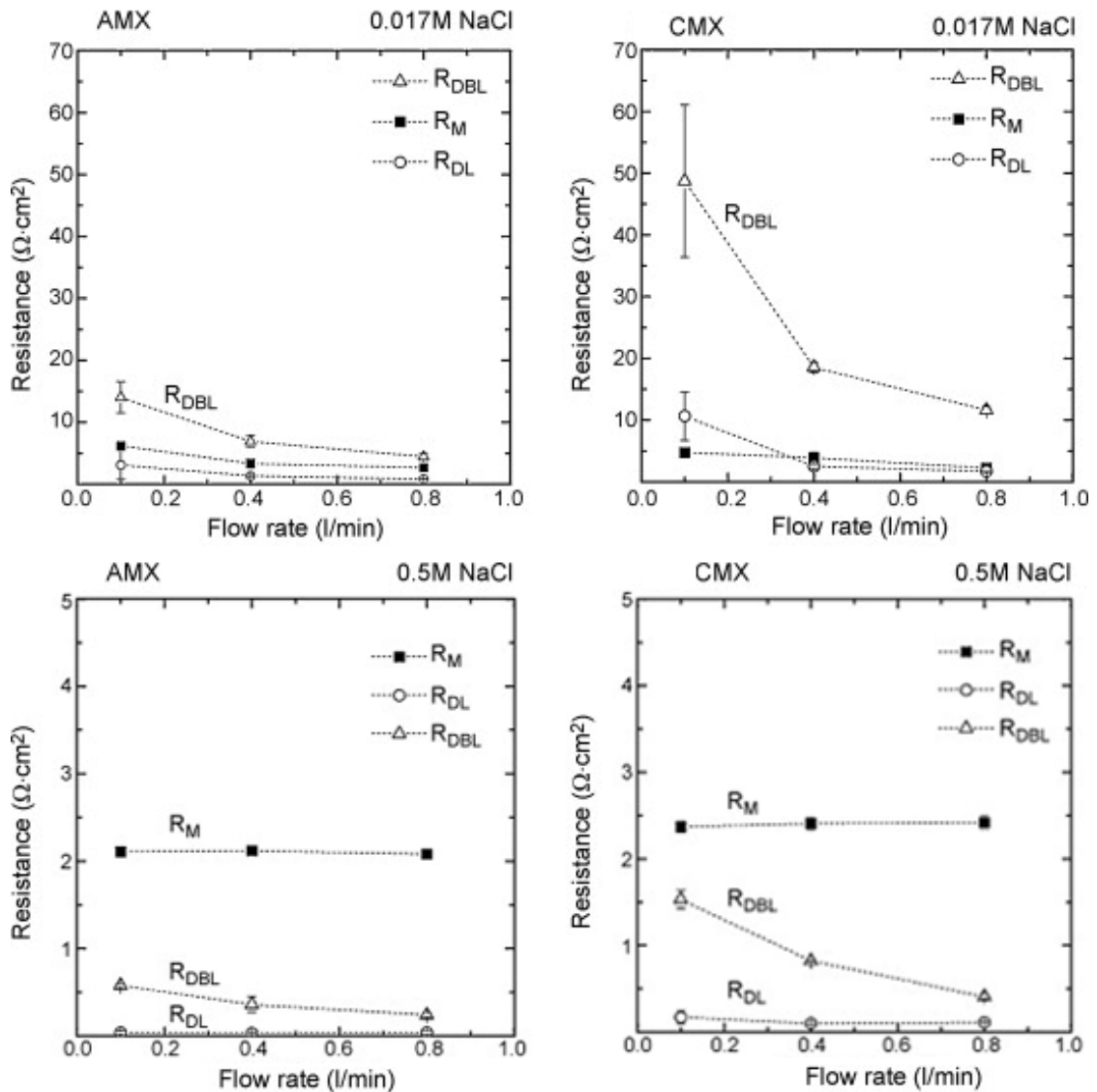
2.2.1 Individual contribution of boundary layers to resistance

The total membrane resistance can be viewed as the sum of the contributions from the membrane, electric double layer and diffusion boundary layer. Since each layer's contribution behaves as an RC circuit with a different time constant, an electrochemical impedance analysis can be used to isolate the individual contribution from each layer.^[9-13]

Figure 2.4 shows the results of electrochemical impedance spectroscopy for an (Neosepta, AMX) anion exchange membrane and a (Neosepta, CMX) cation exchange membrane at different flow rates and salt concentrations.^[14]

Under all of the conditions tested the electric double layer provided a minimal amount of resistance to the overall membrane system, and is unaffected by the hydrodynamics of the system. Since little can be done to change the electric double layer and the contribution to resistance is small, the electric double layer is often ignored when optimizing membrane design.

At low salt concentrations the diffusion boundary layer provides the majority contribution to membrane resistance, while at high concentrations membrane resistance provides the majority contribution to membrane resistance. Furthermore, resistance due to the diffusion boundary layer can be minimized by increasing the flow rate across the membrane surface, while the membrane resistance changes little with solution flow rate. This observation agrees with the theory that increased mixing can be used to minimize resistance from the diffusion boundary layer.



Długolecki *et al.* [14]

Figure 2.4: Resistance of the diffusion boundary layer (DBL), membrane (M) and electric double layer (DL) for AMX and CMX membranes in 0.017 mol L^{-1} NaCl and 0.5 mol L^{-1} NaCl at various flow rates.

2.2.2 Transport numbers

When a current is carried through an electrolytic solution, any available electro-active species will participate in carrying the current from one electrode to another. The transport number (t_i) describes the fraction of current carried by an individual

species i , relative to the total current being passed in the system:

$$t_i = \frac{J_i}{\sum_j J_j} \quad (2.4)$$

where J_i is the flux of species i .

The mobility of an ionic species i (μ_i) describes the terminal velocity (v_i) of the species within a medium when an electric field of strength \mathcal{E} is applied. It turns out the mobility is relatively constant as the electric field changes and can be estimated using stokes law:^[15]

$$\mu_i = \frac{v_i}{\mathcal{E}} = \frac{|z_i| e}{6\pi\eta r} \quad (2.5)$$

where z_i is the charge of species i , e is the charge of an electron, η is the viscosity of the medium, and r is the radius of the ion.

Equation (2.4) can be written using species mobilities and activities (a_i) as:

$$t_i = \frac{|z_i| \mu_i a_i}{\sum_j |z_j| \mu_j a_j} \quad (2.6)$$

which provides a method for estimating the transport number of a species from reported parameters.

For a solution comprised of a single salt, Equation (2.6) simplifies to:

$$t_i = \frac{\mu_i}{\mu_+ + \mu_-} \quad (2.7)$$

The dilute solution mobilities are reported for many ions in water at 25 °C, which allows for Equation (2.6) to be used to quickly estimate transport numbers for a given species at low concentrations, and is often used for approximating

transport numbers at higher concentrations.

2.3 Membrane permselectivity

The selectivity of species a over species b through a membrane ($\alpha_{a/b}$) is defined by the ratio of permeabilities (\mathcal{P}) for species a and b :

$$\alpha_{a/b} = \frac{\mathcal{P}_a}{\mathcal{P}_b} = \frac{K_a}{K_b} \times \frac{D_a}{D_b} \quad (2.8)$$

where K_i is known as the sorption, or solubility coefficient of species i , and D_i is the diffusion coefficient of species i in the membrane. Selectivity describes the degree to which separation between two species occurs, and is an oft-reported parameter for separation membranes.

The permselectivity of an ion exchange membrane (Ψ) is a parameter related to selectivity that describes the ability of an ion exchange membrane to exclude co-ion transport within the membrane. Membrane permselectivity is defined as one minus the ratio of the transport of the co-ion in the membrane phase (\bar{t}_m) to the transport number of the co-ion in the solution phase (t_m):

$$\Psi = 1 - \frac{\bar{t}_m}{t_m} \quad (2.9)$$

For a perfect membrane no co-ions are used to transport current within the membrane such that $\bar{t}_m = 0$ resulting in a permselectivity of one. Conversely, a perfectly imperfect membrane has no change in ion transport between the membrane and the solution such that $\bar{t}_m = t_m$, leading to a permselectivity of zero.

There is often confusion as to the difference between selectivity and permse-

lectivity, as their definitions are similar and the differences in terminology are subtle. Selectivity describes the affinity for one species to transport through the membrane relative to another, and exists for any two species in the system. For example, suppose a cation exchange membrane is exposed to a solution containing a mixture of sodium chloride and potassium chloride. In this case, sodium and potassium transport easily through the membrane while chloride is mostly excluded. In this case however, it is likely that sodium and potassium will interact differently with the polymer, resulting in one ion that is favored over the other. This will result in a slight separation between sodium and potassium and is described by the selectivity of the two compounds.

On the other hand, permselectivity specifically relates to the ability of a membrane to exclude co-ions from the membrane. In the above example, this would be the reduction in chloride transport within the membrane relative to in the bulk solution. While one could still compute a selectivity between sodium and chloride for this membrane, permselectivity specifically describes the overall performance of the ion exchange membrane.

2.4 Specific ion effects

Seawater is often approximated in the laboratory as a sodium chloride solution, however as Table 2.1 shows, sodium and chloride ions only make up 90% of the ionic composition in real seawater. The presence of other ions affects the properties and performance of membranes when operated in multi-ionic systems such as seawater. Multivalent ions at low concentrations have been shown to reduce the stack potential in reverse electrodialysis.^[16,17] For example, the power density of a reverse electrodialysis stack was found to drop more than 40% over

Table 2.1: Ionic composition of seawater.

Cations					Anions				
Ion	Concentration		Molar mass	Mole %	Ion	Concentration		Molar mass	Mole %
	ppm	mmol/kg				ppm	mmol/kg		
Na ⁺	10752	468	23.0	41.8	Cl ⁻	19345	546	35.4	48.8
Mg ⁺²	1295	53.3	24.3	4.76	SO ₄ ⁻²	2701	28.1	96.1	2.51
Ca ⁺²	416	10.4	40.1	0.93	HCO ₃ ⁻	145	2.34	61.0	0.21
K ⁺	390	9.97	39.1	0.89	Br ⁻	66	0.83	79.9	0.08
Sr ⁺²	13	0.091	87.6	0.008	BO ₃ ⁻³	27	0.46	58.8	0.04
					F ⁻	1	0.068	19.0	0.006

Anthoni [19]

24 hr when run with seawater, which was due to both fouling and the impact of multivalent ions.^[18]

2.4.1 Bi-ionic membrane potential

The simplest setup that shows how membranes perform when exposed to multiple salts is the bi-ionic system. Bi-ionic systems consist of a membrane separating two different salt solutions that share common ion (e.g. NaCl and Na₂SO₄). Tran *et al.* [20] looked at bi-ionic systems with a cation exchange membrane separating a LiCl solution from a NaCl solution. By changing the concentrations of LiCl and NaCl, it was determined that increasing the concentration of the more mobile counter-ion (Li⁺) increases selectivity, while increasing the concentration of the less mobile counter-ion (Na⁺) decreases selectivity. This suggests that ion mobility can be related to permselectivity, with more mobile counter-ions having higher permselectivities.

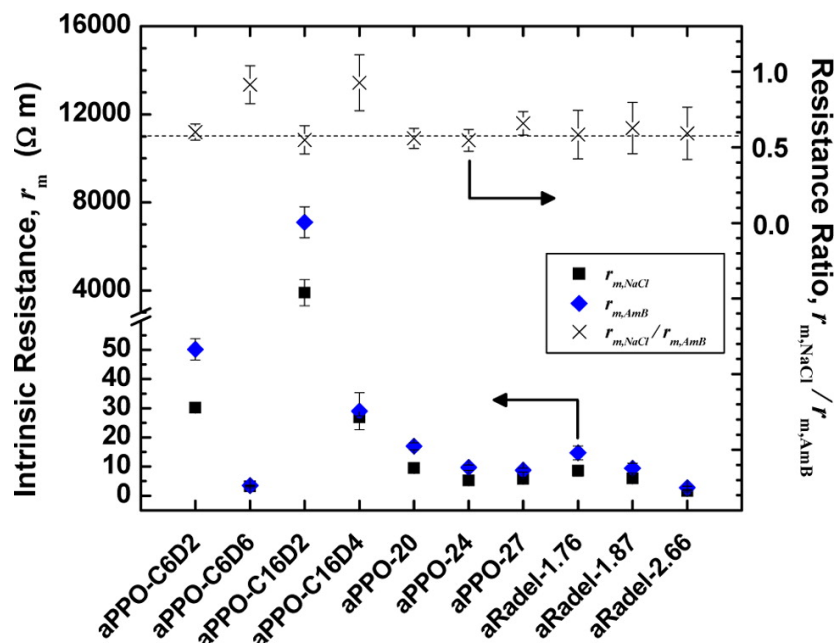
When a membrane separates solutions of multiple ions of differing valencies, a phenomenon called uphill transport can occur. Uphill transport occurs when the increase in entropy caused by exchanging a single higher-valence ion with

multiple lower-valence ions causes the higher-valence ions to travel up a concentration gradient.^[21-26] This results in a bi-ionic potential that resists transport in the direction of the driving force, with even small amounts of divalent and trivalent ions resulting in considerable losses in efficiency. The bi-ionic potential is a major contributor to inefficiencies in real world systems such as seawater.

In order to deal with multivalent solutions and the resultant bi-ionic potential, monovalent permselective membranes, which block the passage of higher-valence ions were developed. Monovalent cation exchange membranes are standard cation exchange membranes with a thin anionic layer either deposited or adsorbed to the surface.^[27-31] Electrostatic repulsion between counter-ions and the anionic layer narrow the point of entry to the membrane, excluding larger divalent ions.^[32] The formation of these cationic layers involves cross-linking near the membrane surface providing additional separation via molecular sieving, since divalent ions tend to be physically larger in hydrated form. While electrostatic repulsion has been confirmed as the major contributor to monovalent selectivity,^[29] cross-linking is assumed to be symbiotic with electrostatic repulsion in improving membrane permselectivity.^[33]

When used in a RED stack, monovalent ion exchange membranes did not provide improvements in power density, although they did provide improved resistance to fouling.^[34] Despite their ineffectiveness at improving RED performance, monovalent ion exchange membranes provide considerable insight into the transport mechanisms occurring within ion exchange membranes.

Geise *et al.* [35] investigated the resistance of anion exchange membranes in single electrolyte sodium chloride, and ammonium bicarbonate solutions. Figure 2.5 shows the resistance of various anion exchange membranes in sodium chloride and ammonium bicarbonate solutions. While the resistance of the dif-



Geise *et al.* [35]

Figure 2.5: Intrinsic resistance of AEMs in 0.5 mol L^{-1} sodium chloride or ammonium bicarbonate. The dashed line represents the ratio of bicarbonate to chloride dilute solution mobilities.

ferent membranes varies considerably, the ratio of resistance between sodium chloride and ammonium bicarbonate was found to equal the ratio of counter-ion dilute solution mobilities for all but two samples.

This observation implies that ion solution mobility can sometimes be used as a probe for ion transport in many ion exchange membranes, however the two outliers demonstrate that other factors can influence the resistance of ion in ion exchange membranes. While ions may behave similar in membranes as they do in solution, care must be taken as ion-membrane interactions may cause deviations from this ideal behavior.

2.4.2 Nanophase separation

The microstructure of a membrane is known to influence ion transport in ion exchange membranes.^[36] Nanophase separation has been found to enhance the conductivity of protons in proton exchange membranes (PEMs).^[37–39]

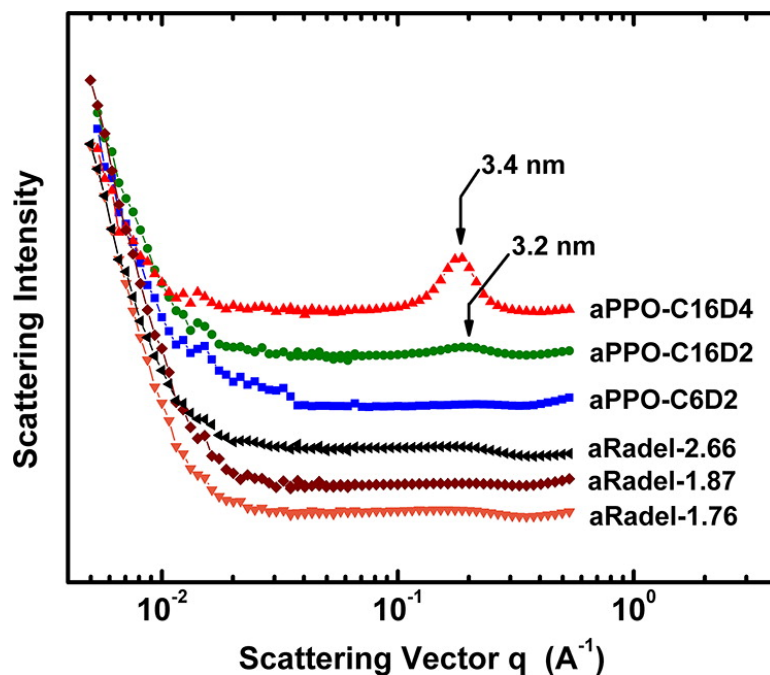
Li *et al.* [40] developed anion exchange membranes with a comb-shaped microstructure by varying the side chain length of the quaternary ammonium functional block. These membranes have highly conductive hydrophilic domains interspersed within hydrophobic domains, which were found to significantly enhance anion conductivity within the membrane.

Small-angle neutron scattering (SANS) performed on the membranes shown in Figure 2.5 show that the two membranes with resistance ratios dissimilar to the predicted ratio exhibit nanophase separation. These two membranes also had significantly higher swelling than the other membranes. This indicates that changing the microstructure of a polymer, as well as changes in the polymer swelling can impact the fundamental mechanisms of ion transport. If the enhanced conductivity was simply due to areas with increased ion exchange content, one would expect the resistance ratio to scale with conductivity. Instead, nanophase separation and polymer swelling were found to enhance the conductivity of the lower-mobility bicarbonate ion versus the higher-mobility chloride ion.

2.5 Membrane upper bound theory

The water uptake of an ion exchange membrane generally increases with an increasing degree of functionalization, as the polymer becomes more hydrophilic.^[41,42]

The free volume element (V_F) of a polymer correlates with the water uptake, with higher water uptake corresponding to larger free volume elements.^[43]



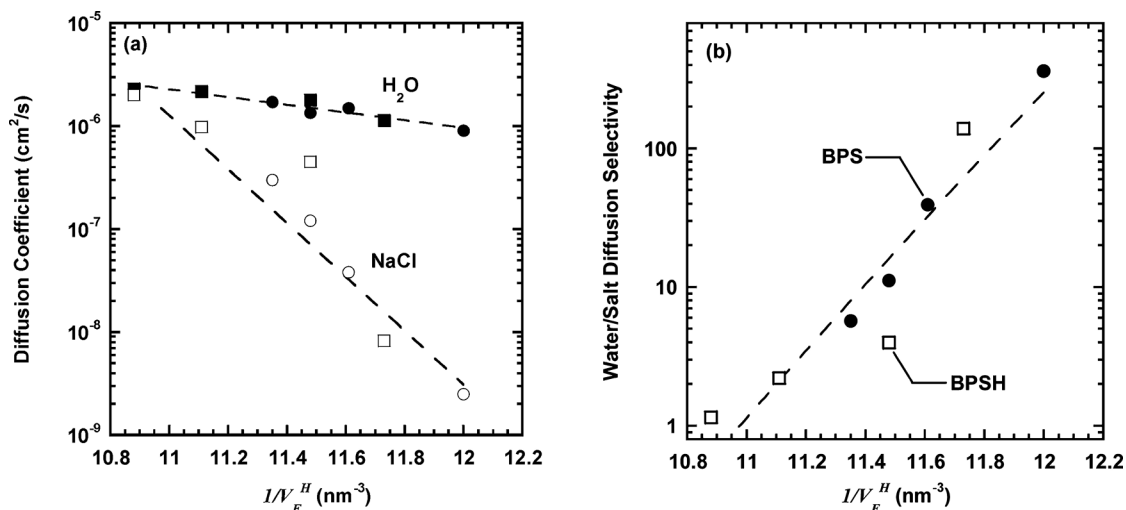
Geise *et al.* [35]

Figure 2.6: Small-angle neutron scattering (SANS) results for membranes shown in Figure 2.5.

Figure 2.7 shows the correlation between free volume element, diffusion coefficient and water/salt selectivity. From a free volume standpoint, membranes with a higher water uptake (high V_F) have higher salt diffusivity and lower selectivity than membranes with a lower water uptake.

The idea that permselectivity and ionic resistance of an ion exchange membrane exhibit an inherent trade-off was expanded on by Geise *et al.* [44]. In this work, Geise *et al.* [44] draws a parallel between the permselectivity/resistance trade-off in ion exchange membranes and the upper bound between permeability and separation factor first observed in gas separation membranes by Robeson [45].

For gas separation membranes, Freeman [46] developed a theoretical model for gas transport in porous membranes. Using this theory, Freeman [46] showed



Xie *et al.* [43]

Figure 2.7: Influence of free volume element size on water and sodium chloride diffusivity and the water/salt selectivity in BPS and BPSH membranes.

that the upper bound is a parameter that can be manipulated using careful membrane and polymer design, and recommended stiffer polymers and increased inter-chain separation to improve the upper bound of gas separation membranes.

2.6 Asymmetric membranes

The development of a comprehensive theory for gas transport in porous membranes by Freeman [46] led to the development of high performance gas separation membranes that raised the limit of the upper bound.^[47] Several methods are used to improve the performance of gas separation membranes, however they all similar in the fact that they involve the creation of thin layers supported by thick non-active layers. These membranes, which have different regions through the cross section of a membrane are called asymmetric membranes, contrast with traditional membranes that are homogeneous throughout. Asymmetric membranes are often used to overcome the upper bound in gas separation membranes, and

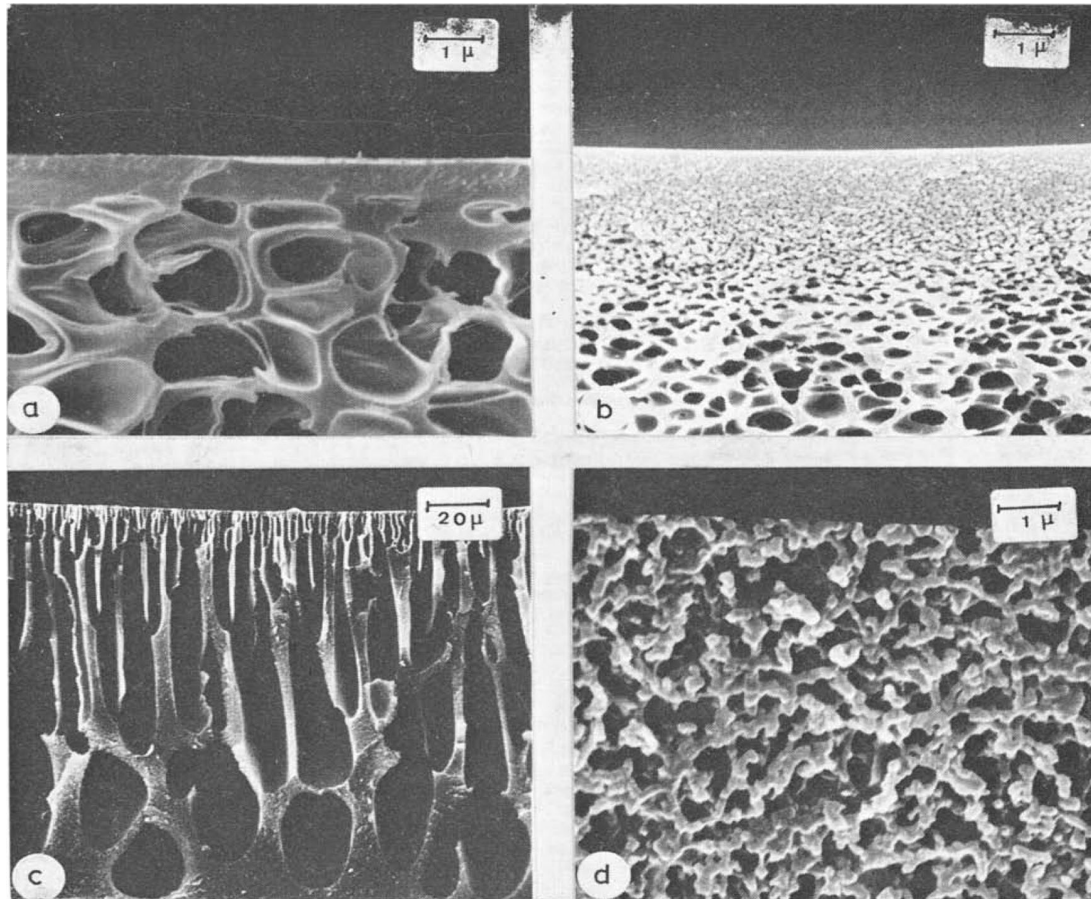
can be prepared by a number of different techniques, including the modification of the membrane surface, phase inversion, spray coating or lamination.

2.6.1 Surface modification

Surface modification of membranes is one commonly used method for the creation of high performance gas separation membranes. One type of surface treatment involves UV irradiation of a membrane surface, which modifies the polymer structure creating a thin layer with a higher selectivity for gas separations.^[48] Membranes surfaces can also be fluorinated, changing the surface energy of the membrane.^[49-51] By influencing the surface energy, selectivity can be achieved in a small region which can produce membranes that beat the initial upper bound first observed by Robeson [45].

2.6.2 Phase inversion

Asymmetric membranes are often prepared by a solubility induced phase inversion. In this process, a polymer is dissolved in a compatible solvent such as dimethylacetamide and spread into a thin film. This thin film is then exposed to an incompatible solvent such as ethanol which quickly precipitates the polymer into a dense layer at the interface of the two phases. This dense layer slows diffusion of the incompatible solvent into the polymer-rich phase, resulting in slower changes of the concentration of the incompatible solvent. Once the process is complete, a thin dense layer has formed upon a thick porous layer, resulting in ideal performance for gas separations. By manipulating variables such as solvent types, concentrations and temperature, a multitude of different structures can be created allowing for a high level of variability in the types of membrane produced, as demonstrated in Figure 2.8.^[52-55]



Strathmann & Kock [53]

Figure 2.8: SEM cross section images showing the different types of membranes structures that can be created using a phase inversion process (a-c) compared to a symmetric porous gas separation membrane (d).

2.6.3 Thin-film composite membranes

A related style of asymmetric membrane that is commonly used for the production of reverse osmosis membranes is the thin-film composite (TFC) membrane. A TFC membrane is a membrane where a thin layer of active material is placed onto a non-active support structure.

There are many methods of producing TFC membranes, but most methods rely on either the preparation of individual layers separately and laminating

them together, depositing a material from a liquid or gas phase onto a substrate, or the reaction of a monomer on the surface of a substrate to build up a layer.^[56] Petersen [57] provides a comprehensive review of different methods that have been used to produce thin film composite membranes.

One key advantage of TFC membranes is that the layers can be characterized independently, and individually tuned for a given performance metric. In other styles of asymmetric membranes, such as those prepared via phase inversion, the porous support structure must be composed of the active material, and is limited to the types of structures that can be created using phase inversion, whereas with TFC membranes, a much wider variety of support materials and structures can be used. Membranes prepared via phase inversion are also limited to polymers that can be dissolved in a solvent and precipitated under specific conditions, whereas TFC membranes can be produced using almost any polymer using a variety of techniques.^[58-60] These factors provide a level of customization not possible with other types of asymmetric membranes, however TFC membranes tend to be thicker and more expensive than other types of membranes.

References

1. Sata, T. *Ion exchange membranes: preparation, characterization, modification and application* (Royal Society of Chemistry, Cambridge, 2004).
2. Cowan, D. A. & Brown, J. H. Effect of turbulence on limiting current in electro dialysis cells. *Industrial & Engineering Chemistry* **51**, 1445–1448 (1959).
3. Rosenberg, N. W. & Tirrell, C. E. Limiting currents in membrane cells. *Industrial & Engineering Chemistry* **49**, 780–784 (1957).
4. Rubinstein, I., Zaltzman, B., Pretz, J. & Linder, C. Experimental verification of the electroosmotic mechanism of overlimiting conductance through a cation exchange electro dialysis membrane. *Russian Journal of Electrochemistry* **38**, 853–863 (2002).
5. Strathmann, H., Krol, J., Rapp, H.-J. & Eigenberger, G. Limiting current density and water dissociation in bipolar membranes. *Journal of Membrane Science* **125**, 123–142 (1997).
6. Krol, J., Wessling, M. & Strathmann, H. Concentration polarization with monopolar ion exchange membranes: current-voltage curves and water dissociation. *Journal of Membrane Science* **162**, 145–154 (1999).
7. Kang, M.-S., Choi, Y.-J. & Moon, S.-H. Effects of charge density on water splitting at cation-exchange membrane surface in the over-limiting current region. *Korean Journal of Chemical Engineering* **21**, 221–229 (2004).
8. Yossifon, G., Mushenheim, P., Chang, Y.-C. & Chang, H.-C. Eliminating the limiting-current phenomenon by geometric field focusing into nanopores and nanoslots. *Physical Review E* **81**, 046301 (2010).
9. Park, J.-S., Choi, J.-H., Woo, J.-J. & Moon, S.-H. An electrical impedance spectroscopic (EIS) study on transport characteristics of ion-exchange membrane systems. *Journal of Colloid and Interface Science* **300**, 655–662 (2006).
10. Coster, H. G. L., Chilcott, T. C. & Coster, A. C. F. Impedance spectroscopy of interfaces, membranes and ultrastructures. *Bioelectrochemistry and Bioenergetics* **40**, 79–98 (1996).

11. Karpenko, L. V. *et al.* Comparative Study of Methods Used for the Determination of Electroconductivity of Ion-Exchange Membranes. *Russian Journal of Electrochemistry* **37**, 287–293 (2001).
12. Chilcott, T. C., Coster, H. G. L. & George, E. P. A novel method for the characterisation of the double fixed charge (bipolar) membrane using impedance spectroscopy. *Journal of Membrane Science* **108**, 185–197 (1995).
13. Park, J. .-S., Chilcott, T. C., Coster, H. G. L. & Moon, S. .-H. Characterization of BSA-fouling of ion-exchange membrane systems using a subtraction technique for lumped data. *Journal of Membrane Science* **246**, 137–144 (2005).
14. Długołęcki, P. *et al.* On the resistances of membrane, diffusion boundary layer and double layer in ion exchange membrane transport. *Journal of Membrane Science* **349**, 369–379 (2010).
15. Bard, A. J. & Faulkner, L. R. *Electrochemical methods: fundamentals and applications* Second (John Wiley & Sons, Inc., New York, NY, 2001).
16. Post, J. W., Hamelers, H. V. & Buisman, C. J. Influence of multivalent ions on power production from mixing salt and fresh water with a reverse electro dialysis system. *Journal of Membrane Science* **330**, 65–72 (2009).
17. Vermaas, D. A., Veerman, J., Saakes, M. & Nijmeijer, K. Influence of multivalent ions on renewable energy generation in reverse electro dialysis. *Energy Environ. Sci.* **7**, 1434–1445 (2014).
18. Vermaas, D. A., Kunteng, D., Saakes, M. & Nijmeijer, K. Fouling in reverse electro dialysis under natural conditions. *Water Research* **47**, 1289–1298 (2013).
19. Anthoni, J. F. *The chemical composition of seawater* Seafriends. url: <http://www.seafriends.org.nz/oceano/seawater.htm> (2006).
20. Tran, S., Dammak, L., Larchet, C. & Auclair, B. Bi-ionic potential through a cation exchange membrane separating two electrolyte solutions at different concentrations. *Electrochimica Acta* **44**, 2515–2521 (1999).
21. Helfferich, F. G. *Ion exchange* (Dover Publications, New York, 1962).
22. Higa, M., Tanioka, A. & Kira, A. Ionic transport against its concentration gradient across bipolar membranes. *Journal of the Chemical Society, Faraday Transactions* **94**, 2429–2433 (1998).
23. Panchenko, L. F., Fedotov, N. S. & Tarshis, M. A. Transport properties of membrane vesicles from *Acholeplasma laidlawii*. II. Kinetic characteristics and specificity of glucose transport system. *Folia Microbiologica* **20**, 480–487 (1975).
24. Wódzki, R., Sionkowski, G. & Poźniak, G. Recovery and concentration of metal ions. IV. Uphill transport of Zn(II) in a multimembrane hybrid system. *Separation Science and Technology* **34**, 627–649 (1999).

25. Cox, J. A. & Poopisut, N. Preconcentration of dopamine by uphill transport across an ion-exchange membrane. *Analytical Chemistry* **64**, 423–426 (1992).
26. Koropchak, J. A. & Allen, L. Flow-injection Donnan dialysis preconcentration of cations for flame atomic absorption spectrophotometry. *Analytical Chemistry* **61**, 1410–1414 (1989).
27. Sata, T. Modification of properties of ion exchange membranes. II. Transport properties of cation exchange membranes in the presence of water-soluble polymers. *Journal of Colloid and Interface Science* **44**, 393–406 (1973).
28. Sata, T. Modification of properties of ion-exchange membranes. IV. Change of transport properties of cation-exchange membranes by various polyelectrolytes. *Journal of Polymer Science: Polymer Chemistry Edition* **16**, 1063–1080 (1978).
29. Sata, T. & Izuo, R. Modification of the transport properties of ion exchange membranes. XII. Ionic composition in cation exchange membranes with and without a cationic polyelectrolyte layer at equilibrium and during electro-dialysis. *Journal of Membrane Science* **45**, 209–224 (1989).
30. Tanaka, Y. Mechanism of low permeability treatment for bivalent ions through an ion exchange membrane. *Journal of the Electrochemical Society of Japan* **42**, 26 (1974).
31. Tanaka, Y. & Senō, M. Treatment of ion exchange membranes to decrease divalent ion permeability. *Journal of Membrane Science* **8**, 115–127 (1981).
32. Sata, T., Izuo, R. & Takata, K. Modification of the transport properties of ion exchange membranes. IX. Layer formation on a cation exchange membrane by acid-amide bonding, and transport properties of the resulting membrane. *Journal of Membrane Science* **45**, 197–208 (1989).
33. Sata, T. Studies on ion exchange membranes with permselectivity for specific ions in electro-dialysis. *Journal of Membrane Science* **93**, 117–135 (1994).
34. Güler, E., van Baak, W., Saakes, M. & Nijmeijer, K. Monovalent-ion-selective membranes for reverse electro-dialysis. *Journal of Membrane Science* **455**, 254–270 (2014).
35. Geise, G. M., Hickner, M. A. & Logan, B. E. Ammonium bicarbonate transport in anion exchange membranes for salinity gradient energy. *ACS Macro Letters* **2**, 814–817 (2013).
36. Kreuer, K.-D. Proton conductivity: materials and applications. *Chemistry of Materials* **8**, 610–641 (1996).
37. Lee, H.-S., Roy, A., Lane, O., Dunn, S. & McGrath, J. E. Hydrophilic-hydrophobic multiblock copolymers based on poly(arylene ether sulfone) via low-temperature coupling reactions for proton exchange membrane fuel cells. *Polymer* **49**, 715–723 (2008).

38. Ghassemi, H., Ndip, G. & McGrath, J. E. New multiblock copolymers of sulfonated poly(4'-phenyl-2,5-benzophenone) and poly(arylene ether sulfone) for proton exchange membranes. II. *Polymer* **45**, 5855–5862 (2004).
39. Wang, H., Badami, A. S., Roy, A. & McGrath, J. E. Multiblock copolymers of poly(2,5-benzophenone) and disulfonated poly(arylene ether sulfone) for proton-exchange membranes. I. Synthesis and characterization. *Journal of Polymer Science Part A: Polymer Chemistry* **45**, 284–294 (2007).
40. Li, N., Yan, T., Li, Z., Thurn-Albrecht, T. & Binder, W. H. Comb-shaped polymers to enhance hydroxide transport in anion exchange membranes. *Energy & Environmental Science* **5**, 7888–7892 (2012).
41. Kimura, S. G. Reverse osmosis performance of sulfonated poly(2,6-dimethylphenylene ether) ion exchange membranes. *Product R&D* **10**, 335–339 (1971).
42. Geise, G. M. *et al.* Water purification by membranes: The role of polymer science. *Journal of Polymer Science Part B: Polymer Physics* **48**, 1685–1718 (2010).
43. Xie, W. *et al.* Effect of free volume on water and salt transport properties in directly copolymerized disulfonated poly(arylene ether sulfone) random copolymers. *Macromolecules* **44**, 4428–4438 (2011).
44. Geise, G. M., Hickner, M. A. & Logan, B. E. Ionic resistance and permselectivity tradeoffs in anion exchange membranes. *ACS Applied Materials & Interfaces* **5**, 10294–10301 (2013).
45. Robeson, L. M. Correlation of separation factor versus permeability for polymeric membranes. *Journal of Membrane Science* **62**, 165–185 (1991).
46. Freeman, B. D. Basis of permeability / selectivity tradeoff relations in polymeric gas separation membranes. *Macromolecules* **32**, 375–380 (1999).
47. Robeson, L. M. The upper bound revisited. *Journal of Membrane Science* **320**, 390–400 (2008).
48. Hsu, K., Nataraj, S., Thorogood, R. & Puri, P. O₂/N₂ Selectivity improvement for polytrimethylsilylpropyne membranes by UV-irradiation and further enhancement by subambient temperature operation. *Journal of Membrane Science* **79**, 1–10 (1993).
49. Le Roux, J., Paul, D., Kampa, J. & Lagow, R. Modification of asymmetric polysulfone membranes by mild surface fluorination Part I: Transport properties. *Journal of Membrane Science* **94**, 121–141 (1994).
50. Le Roux, J., Paul, D., Arendt, M., Yuan, Y. & Cabasso, I. Modification of asymmetric polysulfone membranes by mild surface fluorination Part II: Characterization of the fluorinated surface. *Journal of Membrane Science* **94**, 143–162 (1994).

51. Le Roux, J., Teplyakov, V. & Paul, D. Gas transport properties of surface fluorinated poly (vinyltrimethylsilane) films and composite membranes. *Journal of Membrane Science* **90**, 55–68 (1994).
52. Strathmann, H., Kock, K., Amar, P. & Baker, R. The formation mechanism of asymmetric membranes. *Desalination* **16**, 179–203 (1975).
53. Strathmann, H. & Kock, K. The formation mechanism of phase inversion membranes. *Desalination* **21**, 241–255 (1977).
54. So, M. T., Eirich, F. R., Strathmann, H. & Baker, R. W. Preparation of asymmetric loeb-sourirajan membranes. *Journal of Polymer Science: Polymer Letters Edition* **11**, 201–205 (1973).
55. Frommer, M. A., Matz, R. & Rosenthal, U. Mechanism of formation of reverse osmosis membranes. precipitation of cellulose acetate membranes in aqueous solutions. *Industrial & Engineering Chemistry Product Research and Development* **10**, 193–196 (1971).
56. Cadotte, J. E. & Petersen, R. J. *Thin-Film Composite Reverse-Osmosis Membranes: Origin, Development, and Recent Advances in Synthetic Membranes: 153* (American Chemical Society, 1981), 305–326.
57. Petersen, R. J. Composite reverse osmosis and nanofiltration membranes. *Journal of Membrane Science* **83**, 81–150 (1993).
58. Lau, W. J., Ismail, A. F., Misdan, N. & Kassim, M. A. A recent progress in thin film composite membrane: A review. *Desalination. Special Issue in honour of Professor Takeshi Matsuura on his 75th Birthday* **287**, 190–199 (2012).
59. Yip, N. Y., Tiraferri, A., Phillip, W. A., Schiffman, J. D. & Elimelech, M. High Performance Thin-Film Composite Forward Osmosis Membrane. *Environmental Science & Technology* **44**, 3812–3818 (2010).
60. Harisha, R. S., Hosamani, K. M., Keri, R. S., Nataraj, S. K. & Aminabhavi, T. M. Arsenic removal from drinking water using thin film composite nanofiltration membrane. *Desalination* **252**, 75–80 (2010).

Chapter 3 |

Specific Ion Effects on the Permselectivity of Sulfonated Poly(Ether Sulfone) Cation Exchange Membranes*

3.1 Introduction

With processes such as RED, redox flow batteries, fuel cells, desalination and ionic separations utilizing a multitude of salts, understanding how membrane permselectivity changes for salts other than sodium chloride (in which ion exchange membranes are typically characterized)^[1,2] is crucial for the success of ion-exchange based energy technologies.

For ammonium bicarbonate processes, Geise *et al.* [3] found that both co- and counter-ion identity affects permselectivity for commercial cation and anion exchange membranes. For Selemion CMV commercial membranes, permselectivity was governed by the counter-ion binding affinity to the fixed ion group, with lower binding affinity resulting in a higher permselectivity. For both Selemion AMV and CMV membranes, co-ion charge density and polarizability was found to govern permselectivity, with co-ions with high charge densities and low polarizabilities having higher permselectivities. In general, previous studies

*This chapter has been adapted from: Cassady, H. J., Cimino, E. C., Kumar, M. & Hickner, M. A. Specific ion effects on the permselectivity of sulfonated poly(ether sulfone) cation exchange membranes. *Journal of Membrane Science* **508**, 146-152 (2016).

have focused on commercial membranes for which the membrane properties are unknown and cannot be tuned, and salts that tend to have high levels of speciation.^[3-5]

In this work, I focused on sulfonated poly(ether sulfone) (SPES) cation exchange membranes with a wide range of functionalization equilibrated with lithium chloride, sodium chloride, potassium chloride, lithium sulfate, sodium sulfate and potassium sulfate. These model materials and salts were used to systemically investigate the co-ion and counter-ion effects on permselectivity in cation exchange membranes where no speciation effects were present in the salts studied. Membrane permselectivity and water uptake were measured to investigate the effect of changing electrolytes on membrane performance.

3.2 Materials and methods

3.2.1 Ion exchange membranes

Cation exchange membranes were prepared by casting sulfonated poly(ether sulfone) (SPES) dissolved in dimethylacetamide (DMAc) with a polymer mass fraction of 4 % into square glass molds with a target thickness of 100 μ m. The membranes were dried under atmospheric pressure at 80 °C for 24 h, and then placed under vacuum at 60 °C for another 24 h to ensure complete evaporation of DMAc. The SPES polymer used was the Aquafone SES01 Series (YANJIN Technology, Tianjin, China), and were purchased with five degrees of functionalization as summarized in Table 3.1. Membranes equilibrated in 0.5 M solutions of the test salt for at least 24 h, changing the solution at least three times.

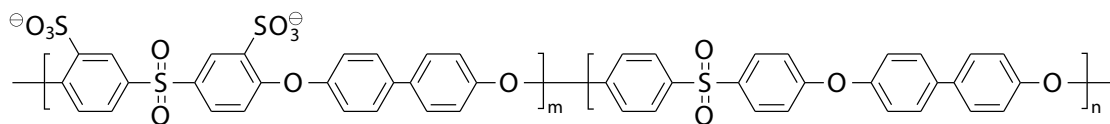


Figure 3.1: Chemical structure of sulfonated poly(ether sulfone) used in this research. The ratio of functionalized to unfunctionalized repeat units represents the degree of functionalization: d.f. = $m/(n + m)$.

Table 3.1: Properties of the sulfonated poly(ether sulfone) polymers used in this study.

Degree of functionalization	IEC ^a [meq/g drypolymer]	Water uptake ^{b,c} [g water/g drypolymer]					
		LiCl	NaCl	KCl	Li ₂ SO ₄	Na ₂ SO ₄	K ₂ SO ₄
20%	0.92	0.20(4)	0.14(3)	0.14(2)	0.13(1)	0.16(2)	0.14(1)
30%	1.34	0.28(2)	0.21(2)	0.26(5)	0.19(3)	0.20(3)	0.22(2)
40%	1.72	0.44(2)	0.33(1)	0.31(1)	0.28(1)	0.40(2)	0.30(3)
50%	2.08	0.65(3)	0.45(3)	0.46(7)	0.34(2)	0.45(3)	0.37(4)
60%	2.42	0.77(7)	0.65(3)	0.55(7)	0.47(3)	0.76(5)	0.50(2)

^a From manufacturer specifications.

^b Measured at room temperature with a solution concentration of 0.5 mol L⁻¹.

^c An uncertainty of one standard deviation is represented in brackets.

3.2.2 Water uptake

Water uptake (w_u) is defined as the mass of water absorbed by a polymer divided by the dry mass of the polymer:

$$w_u = \frac{m_{\text{swollen}} - m_{\text{dry}}}{m_{\text{dry}}} \quad (3.1)$$

Water uptake was found by measuring mass of a swollen membrane sample immediately after blotting off surface water. The membrane sample was then allowed to dry under vacuum at 60 °C before measuring the dry mass of the polymer.

3.2.3 Permselectivity

Theory

An electric diffusion potential develops to balance the entropic force driving ions from the ionomer to the solution. The general Nernst equation for a membrane concentration potential describes this diffusion potential:^[6]

$$E_{\text{diff}} = -\frac{RT}{F} \int \sum \frac{t_i}{z_i} d \ln a_i \quad (3.2)$$

where R is the ideal gas constant, T is the absolute temperature, F is Faraday's constant, z_i is the charge number of ion i , t_i is the transport number (the fraction of current carried by a species) of ion i , and a_i is the effective concentration (activity) of ion i .

A similar equation describes the electric potential across the interface of a charged polymer when exposed to an ionic solution. This Donnan potential is described by:

$$E_{\text{don}} = \bar{\psi} - \psi = \frac{1}{z_i F} \left[RT \ln \frac{a_i}{\bar{a}_i} - (\bar{P} - P) V_i \right] \quad (3.3)$$

where V_i represents the partial molar volume of ion i , and a bar over a variable represents a membrane phase property and the absence of one represents a solution phase property. Equation (3.3) is equivalent for all ions in the system.

For a single salt with negligible swelling pressure, applying the condition of electroneutrality to Equation (3.3) results in the Donnan membrane equilibrium equation:

$$\bar{a}_m^{v_m} \bar{a}_x^{v_x} = a_m^{v_m} a_x^{v_x} \quad (3.4)$$

where ν_m and ν_x are the stoichiometric coefficients of the co- and counter-ion, respectively. Since the right hand side of Equation (3.4) is set for a given salt solution, the high membrane phase counter-ion activity (\bar{a}_x) needed to balance the large number of fixed ion groups results in a low membrane phase co-ion activity (\bar{a}_m). This reduction in membrane phase co-ion activity is the mechanism behind the permselective properties for an ion exchange polymer.

Membrane permselectivity describes the degree to which ion exchange membrane excludes co-ions:

$$\Psi = 1 - \frac{\bar{t}_m}{t_m} \quad (3.5)$$

A perfect membrane has no co-ion transport and hence a permselectivity of one, while a membrane with no ionic selectivity transports co-ions at the same rate as the solution and has a permselectivity of zero.

Ion transport numbers can be determined by measuring the potential of a membrane separating solutions of different concentrations and using Equations (3.2) and (3.3). These transport numbers can be inserted into Equation (3.5) to give membrane permselectivity.

To determine ion transport numbers using Equation (3.2), one must know the activities of each ion in solution, which are not typically known; usually only the mean salt activity is reported. For instance, the activity coefficient of NaCl in a 1.1 mol L^{-1} aqueous solution is 0.650, but the activity coefficient of the Na^+ cation is 0.747 and the activity coefficient of the Cl^- anion is 0.564.^[7] For a membrane separating two solutions of the same salt with different mean activities ($a'_\pm > a''_\pm$), the ratio of mean activities can be related to the ratio of individual anion and cation activities by:

$$\frac{a''_+}{a'_+} = \frac{a''_-}{a'_-} = \frac{a''_\pm}{a'_\pm} \quad (3.6)$$

for a 1:1 salt.^[8] This relation causes the individual ion activities to simplify to mean salt activities, resulting in the permselectivity equations most often reported. To determine permselectivity for membranes in salts that are not 1:1, a different method for relating individual ion activities to mean salt activities must be employed.

To relax the 1:1 salt requirement, a method developed by Harper [9] for relating the activity coefficient of an individual ion (γ_+ or γ_-) to the activity coefficient of its neutral salt (γ_{\pm}) can be used. By convention, the mean activity coefficient of a salt is defined as:

$$\gamma_{\pm} = \gamma_+^{v_+} \gamma_-^{v_-} \quad (3.7)$$

Harper [9] provides several substitutions that allow Equation (3.7) to be rearranged to give:

$$\gamma_+ = \gamma_{\pm}^{\frac{z_+^2}{|z_+ + z_-|}} \quad \text{and} \quad \gamma_- = \gamma_{\pm}^{\frac{z_-^2}{|z_+ + z_-|}} \quad (3.8)$$

The membrane potential (φ_m) of a membrane separating two solutions of different concentration ($a' > a''$) is the sum of the Donnan potential at the high (E'_{don}) and the low (E''_{don}) concentration interface, as well as the diffusion potential in the polymer phase (\bar{E}_{diff}):

$$\varphi_m = E'_{\text{don}} + \bar{E}_{\text{diff}} + E''_{\text{don}} \quad (3.9)$$

At equilibrium the electrochemical potential of a species is continuous across a phase boundary.^[10] Applying this concept at each of the membrane interfaces provides a relation between the activities for a species across the membrane

surfaces under equilibrium conditions:^[11]

$$\frac{\bar{a}'_i}{\bar{a}''_i} = \frac{a'_i}{a''_i} \quad (3.10)$$

This means that $E'_{\text{don}} = -E''_{\text{don}}$, and the membrane potential equals the diffusion potential. Assuming ion transport numbers are not a function of activity, Equation (3.2) can be integrated for a binary salt to give:

$$\varphi_m = \frac{RT}{F} \left[-\frac{\bar{t}_+}{z_+} \ln \left(\frac{a''_+}{a'_+} \right) + \frac{\bar{t}_-}{z_-} \ln \left(\frac{a''_-}{a'_-} \right) \right] \quad (3.11)$$

Combining Equations (3.8) and (3.11) gives the membrane potential, which in cation form is:

$$\varphi_m = -\frac{RT}{F} \left\{ \left[\frac{z_+ + z_-}{z_+ z_-} \ln \left(\frac{a''}{a'} \right) \right] \bar{t}_+ - \ln \left[\left(\frac{\gamma''_{\pm}}{\gamma'_{\pm}} \right)^{\frac{1}{z_+}} \left(\frac{C''}{C'} \right)^{\frac{1}{z_-}} \right] \right\} \quad (3.12)$$

An analogous and equivalent anion form of Equation (3.11) can also be derived.

For a perfectly permselective membrane, $\bar{t}_m = 1$ and $\bar{t}_x = 0$, which can be applied to Equation (3.12) to give the membrane potential for an ideal membrane:

$$\varphi_{m,sp} = -\frac{RT}{F} \ln \left[\left(\frac{\gamma''_{\pm}}{\gamma'_{\pm}} \right)^{\frac{1}{z_x}} \left(\frac{C''}{C'} \right)^{\frac{1}{z_m}} \right] \quad (3.13)$$

Combining Equations (3.5), (3.12) and (3.13) gives the permselectivity for an ion exchange membrane as a function of measured membrane potential:

$$\Psi = \frac{n}{d} \quad (3.14)$$

Table 3.2: Mean activity coefficients used for salts at different concentrations.

Concentration [mol kg ⁻¹]	Mean activity coefficient ^[14]					
	LiCl	NaCl	KCl	Li ₂ SO ₄	Na ₂ SO ₄	K ₂ SO ₄
0.1	0.790	0.778	0.770	0.478	0.452	0.436
0.5	0.739	0.681	0.649	0.326	0.270	0.261

where

$$n = \left\{ \left(\frac{\varphi_m}{\varphi_{m,sp}} \right) \ln \left[\left(\frac{\gamma''_{\pm}}{\gamma'_{\pm}} \right)^{z_m} \left(\frac{C''}{C'} \right)^{z_x} \right] \right\} +$$

$$\ln \left[\left(\frac{\gamma''_{\pm}}{\gamma'_{\pm}} \right)^{z_x} \left(\frac{C''}{C'} \right)^{z_m} \right] - (z_m + z_x) \ln \left(\frac{a''}{a'} \right) t_m$$

$$d = (z_m + z_x) \ln \left(\frac{a''}{a'} \right) t_x$$

For a 1:1 monovalent electrolyte, $z_m = z_x = 1$, which reduces Equation (3.14) to:

$$\Psi = \frac{\frac{\varphi_m}{\varphi_{m,sp}} + 1 - 2t_m}{2t_x} \quad (3.15)$$

which is the commonly reported equation defining membrane permselectivity in a 1:1 electrolyte.^[12]

The transport number of an ion in a single salt solution is related to ion mobilities (μ_i) by:^[13]

$$t_i = \frac{\mu_i}{\mu_+ + \mu_-} \quad (3.16)$$

The dilute solution mobility values reported in Table 3.4 were used with Equation (3.16) to determine the solution transport numbers needed to compute permselectivity in Equation (3.14). The activity coefficients used in Equation (3.14) for computing permselectivity are reported in Table 3.2.

Membrane potential

Membrane potential was measured using the device shown in Figure 3.2. A high concentration (0.5 mol L^{-1}) and a low concentration (0.1 mol L^{-1}) solution is pumped on either side of the membrane. The solutions are configured in a single pass setup at a flow rate of 5 mL min^{-1} . An overhead mixer at 550 rpm stirred each compartment. The system is allowed to reach equilibrium by waiting until the average measured potential across two silver/silver chloride double junction reference electrodes stabilizes to 0.1 mV (at least 20 min, sometimes up to 2 h). Once equilibrium is obtained, the potential across the reference electrodes is averaged over the span of approximately 15 min to give the measured membrane potential. The time to reach equilibrium varied significantly, even for the same membrane/salt pair. The unpredictable equilibration time is most likely due to the reference electrodes adjusting to the test environment. However, differences in equilibration times were not found to affect repeatability of the measured membrane potential. The offset between the two electrodes is measured in a 0.5 mol L^{-1} solution of the salt being tested and subtracted from the measured membrane potential giving the final, corrected membrane potential.

3.3 Results and Discussion

3.3.1 Water uptake

When an ion-functionalized polymer is placed in water and begins to swell, the fixed ionic groups are diluted. Donnan theory predicts that a reduction in fixed charge concentration lowers ionic exclusion, which would lead to a reduced permselectivity as water uptake increases. Therefore, water uptake is often used

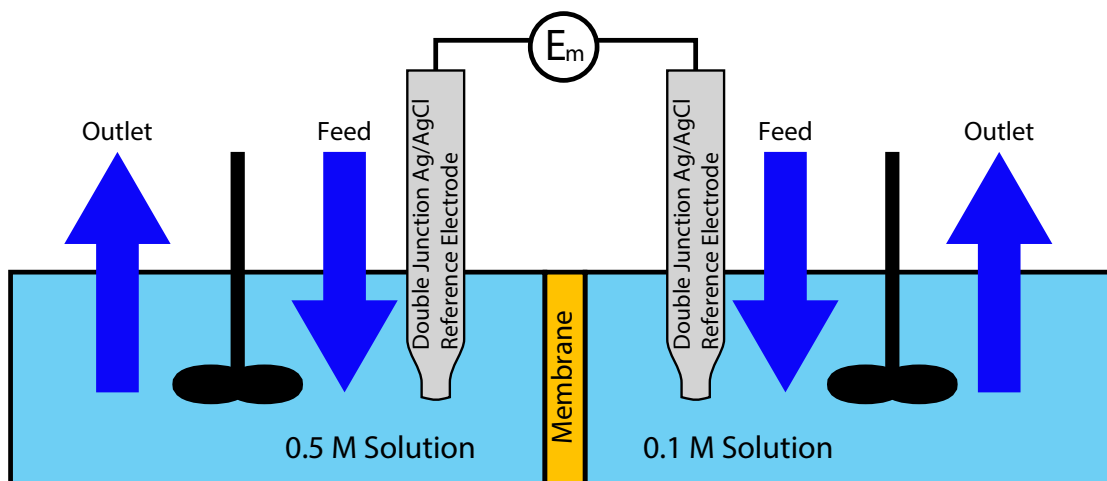


Figure 3.2: Cell for measuring membrane potential for a membrane subject to a concentration gradient. The electrodes are placed 1 cm from the membrane surface and the membrane area is 10 cm^2 .

as a simple descriptor for estimating membrane permselectivity where higher water uptake membranes generally have lower permselectivity.

Permselectivity and water uptake was measured as shown in Figure 3.3. For a given salt, permselectivity is lower for more highly functionalized membranes that have higher water uptakes as predicted by swelling and Donnan theory.^[15] However, the permselectivity of different salts varies greatly for membranes with the same degree of functionalization and similar water uptake. For instance, for a membrane with $d.f. = 0.4$, the water uptake in NaCl and K_2SO_4 is similar at $0.33(1) \text{ g}_{\text{water}}/\text{g}_{\text{polymer}}$ and $0.30(3) \text{ g}_{\text{water}}/\text{g}_{\text{polymer}}$, respectively, however the permselectivity varies significantly from $0.980(3)$ to $0.79(2)$. Because different salts show drastically different permselectivity values for the same membrane with nearly the same water uptake, specific interactions between the ions and the polymer and the properties of the ions themselves must be examined to uncover the origins of specific ion effects.

Table 3.3 summarizes permselectivity for SPES membranes with a 40% degree

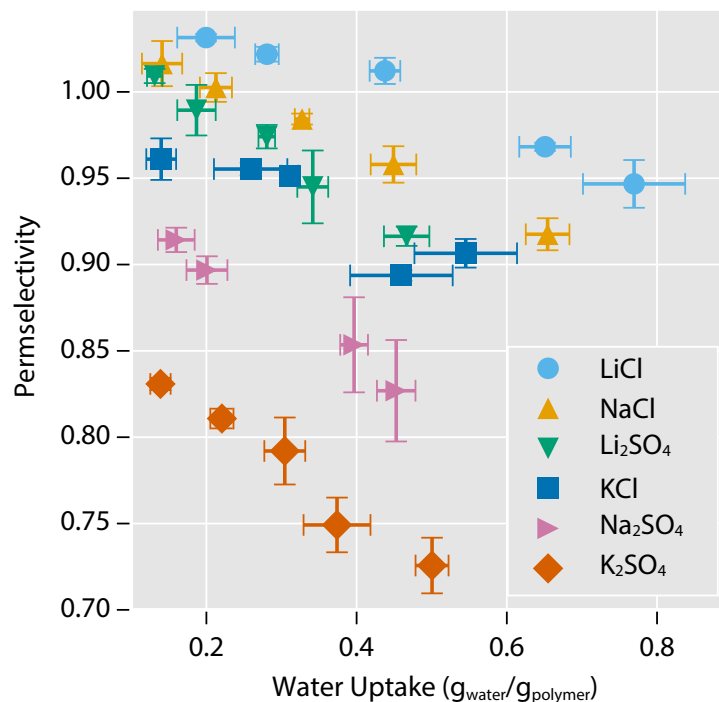


Figure 3.3: Permeability versus water uptake for SPES cation exchange membranes in lithium chloride, sodium chloride, potassium chloride, lithium sulfate, sodium sulfate and potassium sulfate.

of functionalization; one of the five membrane types tested. Permeability was measured for the six electrolytes summarized in Table 3.3. This allows counter-ion effects on permeability (rows in Table 3.3) and co-ion effects on permeability (columns in Table 3.3) to be examined separately. For solutions with different counter-ions, permeability decreased in the order of lithium, sodium and potassium salt solutions. For solutions with different co-ions, chloride salt solutions were found to give a higher permeability than sulfate salt solutions. These trends of counter-ion and co-ion permeability for the 40% sulfonated SPES membrane were representative for all of the SPES membranes studied in this work.

Table 3.3: Permselectivity data for SPES CEM membrane with a 40 % degree of functionalization. Uncertainty is reported as one standard deviation.

		Cations		
		Li ⁺	Na ⁺	K ⁺
Anions	Cl ⁻	1.012(8)	0.984(3)	0.951(4)
	SO ₄ ²⁻	0.974(7)	0.85(3)	0.79(2)

Table 3.4: Properties of the cations and anions considered in this study.

Ion	Hydrated radii ^[16] [Å]	Charge density ^a [e ⁻ /nm ³]	Dilute solution mobility ^[13] [cm ² /S V]	Polarizability [au]	Binding affinity ^[17]
Li ⁺	3.82	4.28	4.01 × 10 ⁻⁴	0.19 ^[18]	1.00
Na ⁺	3.58	5.20	5.19 × 10 ⁻⁴	1.00 ^[18]	1.98
K ⁺	3.31	6.58	7.62 × 10 ⁻⁴	5.40 ^[18]	2.90
Cl ⁻	3.32	6.52	7.91 × 10 ⁻⁴	22.3 ^[19]	
SO ₄ ²⁻	3.79	8.77	8.27 × 10 ⁻⁴	47.2 ^[20]	

^a Calculated from the hydrated radii.

3.3.2 Counter-ion effects on permselectivity

Specific counter-ion effects describe the scenario in which the counter-ion is varied with a constant co-ion (e.g. NaCl and KCl for a CEM). This corresponds to the individual plots in Figure 3.4, where Figure 3.4 (a) represents the chloride co-ion form and Figure 3.4 (b) represents the sulfate co-ion form. The properties of the specific ions examined including size, polarizability, and binding affinity are included in Table 3.4.

Binding affinity describes the proclivity for a cation-anion pair to form a bond. This is related to the equilibrium coefficient such that for salt AB,

$$\text{Binding affinity} \propto \frac{[AB]}{[A^{a+}][B^{b-}]} \quad (3.17)$$

As the binding affinity between a counter-ion and the fixed ion increases, the ratio

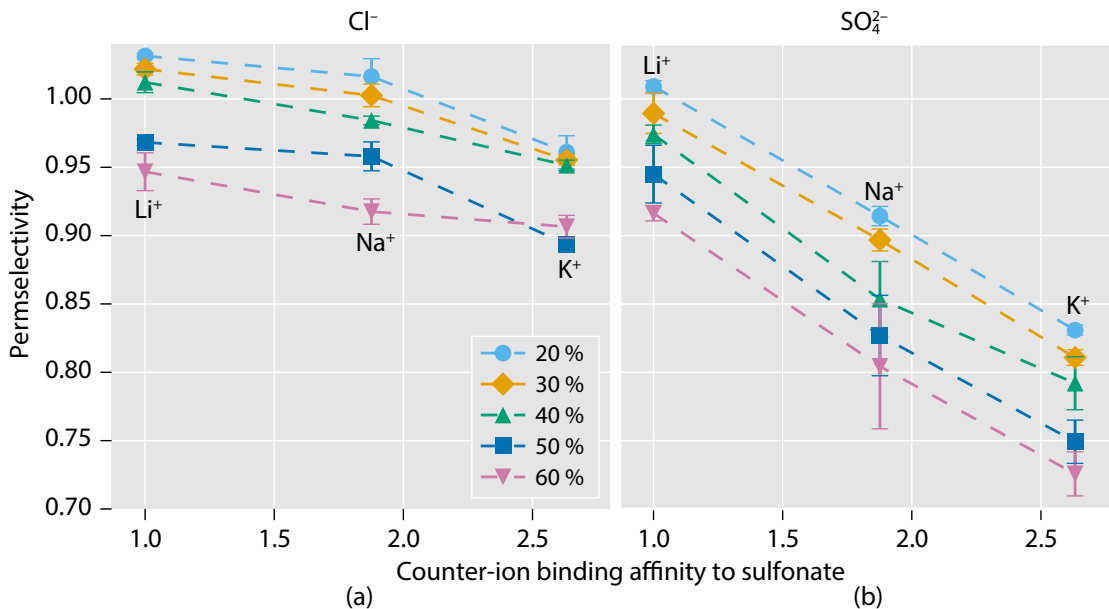


Figure 3.4: Permselectivity versus counter-ion binding affinity for SPES CEMs with five degrees of functionalization: 20 %, 30 %, 40 %, 50 % and 60 % in six different salts, where (a) shows chloride co-ion salts and (b) shows sulfate co-ion salts. Looking at the difference for a specific counter-ion between (a) and (b) shows the effect of changing the co-ion form on permselectivity.

in Equation (3.17) will shift towards condensed counter-ion/fixed-charge pairs as illustrated in Figure 3.5. This counter-ion condensation lowers the concentration of mobile counter-ions within the membrane, which reduces co-ion exclusion as per the Donnan equilibrium.^[21]

Figure 3.4 shows the relation between permselectivity and the counter-ion/fixed-charge pair binding affinity. For both chloride and sulfate co-ions, permselectivity decreases with increasing counter-ion/fixed-charge pair binding affinity, supporting the theory that counter-ion condensation lowers the fixed charge concentration of the membrane.

The effects of counter-ion size and polarizability must also be taken into account. Permselectivity was found to decrease with decreasing counter-ion size, and increase with increasing counter-ion polarizability. While it is currently

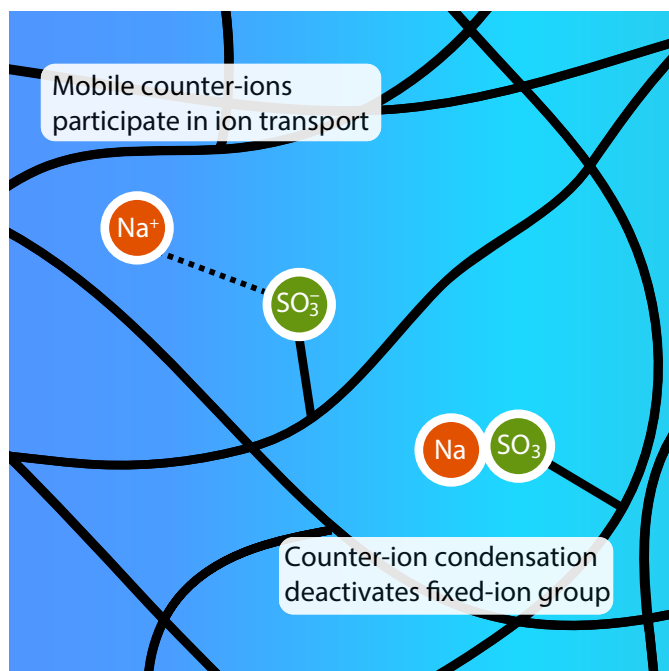


Figure 3.5: Counter-ion interactions with the fixed charge group. Counter-ions can exist either as a solvated pair with the fixed ion group (Na^+ and $\text{R}-\text{SO}_3^-$), or in a condensed salt form (NaSO_3-R). A higher binding affinity increases the fraction of condensed salt pairs, deactivating these sites from transport.

believed that binding affinity is the primary factor impacting permselectivity, it is possible that these properties also contribute to the differences in permselectivity among the counter-ions studied. However, there is no clear theoretical framework to describe specific ion effects using these properties of the ions, which is an area of future development. For example, dilute solution mobility is often used to predict transport properties in membranes,^[4] however Equation (3.5) predicts higher counter-ion mobilities would provide higher permselectivity values, which is opposite from what is observed.

3.3.3 Co-ion effects on permselectivity

The data in Figure 3.4 (a) and Figure 3.4 (b) shows permselectivity for chloride co-ions on the left and sulfate co-ions on the right, for lithium, sodium and potassium

counter-ions. For all three counter-ions tested, membranes with chloride co-ions in solution displayed higher permselectivities than membranes with sulfate co-ions in solution.

Geise *et al.* [3] proposed that a higher co-ion charge density results in higher permselectivity. While co-ion charge density might predict permselectivity between co-ions of the same valence, Table 3.4 shows that this does not hold between the monovalent chloride ion and the divalent sulfate ion. Sulfate has a higher charge density than chloride and therefore sulfate-based salts would be expected to show a higher permselectivity than chloride-based salts if more charge-dense co-ions are excluded from the membrane more readily. The hydrated radius of sulfate is also greater than chloride, which would tend to suggest that it should be excluded from the membrane to a greater extent. Finally, the Donnan equilibrium described in Equation (3.4) would predict that a divalent co-ion has greater exclusion than a monovalent co-ion. This discrepancy between Donnan theory and the experimental observations of Cl^- and SO_4^- permselectivity shows the limitations of the field's current understanding of co-ion transport in ion exchange membranes.

The polarizability of an ion describes the ability of an electric field to influence the charge distribution of an ion. The fixed ionic groups in an ion exchange polymer can more strongly influence more polarizable co-ions, potentially allowing more absorption of high polarizability species into the membrane. Therefore, the more polarizable sulfate co-ion would be expected to have a lower permselectivity than the less polarizable chloride ion (Table 3.4).

It is possible that there are interactions between the effect of the co-ion and counter-ion on permselectivity. For example, a high level of counter-ion condensation would provide less fixed charge sites to influence co-ion charge distribution.

Membrane permselectivity is not currently known for enough salts to determine interaction effects, however a future study could be designed to investigate co-ion and counter-ion interactions using an ANOVA analysis.

Some of the permselectivity values measured were above the theoretical maximum value of unity as seen in Figure 3.4. Since the trend in membrane permselectivity for different IECs and a given salt line up as expected, this is believed to be a systemic shift of the data, possibly due to an uncontrolled experimental variable. For example, it is assumed that the electrode offset measured in a 0.5 mol L^{-1} solution is representative of the electrode offset for the system being tested in 0.5 mol L^{-1} and 0.1 mol L^{-1} solutions. This would not take into account slight differences in the liquid-junction potential at the electrode interface for different solution concentrations, potentially influencing the data. Experiments were also run at temperatures up to $25 \text{ }^\circ\text{C}$, slightly higher than the $20 \text{ }^\circ\text{C}$ for which activity coefficients are reported in the literature. Since Equation (3.14) relies only on the ratio of activity coefficients, a strong temperature dependence on permselectivity is not expected, however if the temperature dependence of activity coefficient on concentration were strong enough, different experimental temperatures could introduce some amount of offset to the data.

While the measured permselectivity might not be valid as an absolute number, the differences and trends for different parameters are still valid. Therefore the given analysis relies only on the differences in permselectivities, not the absolute permselectivity.

3.4 Conclusions

Water uptake and permselectivity was measured for five SPES cation exchange membranes in six different salt solutions in order to isolate the specific effect of both counter-ions and co-ions on membrane permselectivity. Membrane permselectivity correlated with both the co-ion and counter-ion used. For counter-ions, the membrane permselectivity ranked Li^+ , Na^+ , K^+ , from high permselectivity to low, while for counter-ions membrane permselectivity ranked Cl^- , SO_4^{2-} , from high permselectivity to low.

Water uptake and fixed charge density were not found to describe permselectivity effects for different salts, meaning specific interactions between the ions and the polymer govern membrane performance for ion exchange membranes. Strong interactions between counter-ion and fixed charge group (binding affinity) were found to result in counter-ion condensation, leading to lower membrane permselectivity. The ability of the fixed ion group to influence the charge density of the co-ion was found to influence permselectivity, with more polarizable co-ions providing lower membrane permselectivities. Interaction effects between the co-ion and counter-ion were not able to be determined, however future studies will investigate this possibility further.

References

1. Długołęcki, P., Nymeijer, K., Metz, S. & Wessling, M. Current status of ion exchange membranes for power generation from salinity gradients. *Journal of Membrane Science* **319**, 214–222 (2008).
2. Greenlee, L. F., Lawler, D. F., Freeman, B. D., Marrot, B. & Moulin, P. Reverse osmosis desalination: Water sources, technology, and today's challenges. *Water Research* **43**, 2317–2348 (2009).
3. Geise, G. M., Cassady, H. J., Paul, D. R., Logan, B. E. & Hickner, M. A. Specific ion effects on membrane potential and the permselectivity of ion exchange membranes. *Physical Chemistry Chemical Physics* **16**, 21673–21681 (2014).
4. Geise, G. M., Hickner, M. A. & Logan, B. E. Ammonium bicarbonate transport in anion exchange membranes for salinity gradient energy. *ACS Macro Letters* **2**, 814–817 (2013).
5. Geise, G. M., Curtis, A. J., Hatzell, M. C., Hickner, M. A. & Logan, B. E. Salt concentration differences alter membrane resistance in reverse electro dialysis stacks. *Environmental Science & Technology Letters* **1**, 36–39 (2014).
6. Matthews, G. G. *Cellular physiology of nerve and muscle* 4th ed (Blackwell Pub, Osney Mead, Oxford ; Malden, MA, 2003).
7. Zhuo, K., Dong, W., Wang, W. & Wang, J. Activity coefficients of individual ions in aqueous solutions of sodium halides at 298.15 K. *Fluid Phase Equilibria. Special Section: 4th Fluid Properties Challenge* **274**, 80–84 (2008).
8. Sata, T. *Ion exchange membranes: preparation, characterization, modification and application* (Royal Society of Chemistry, Cambridge, 2004).
9. Harper, H. W. Calculation of liquid junction potentials. *The Journal of Physical Chemistry* **89**, 1659–1664 (1985).
10. Koretsky, M. D. *Engineering and chemical thermodynamics* First (Wiley, Hoboken, NJ, 2004).
11. Helfferich, F. G. *Ion exchange* (Dover Publications, New York, 1962).
12. Strathmann, H. *Introduction to membrane science and technology* (Wiley-VCH Verlag & Co., Weinheim, Germany, 2011).

13. Bard, A. J. & Faulkner, L. R. *Electrochemical methods: fundamentals and applications* Second (John Wiley & Sons, Inc., New York, NY, 2001).
14. Robinson, R. A. *Electrolyte solutions* 2nd rev. ed (Dover Publications, Mineola, NY, 2002).
15. Geise, G. M., Paul, D. R. & Freeman, B. D. Fundamental water and salt transport properties of polymeric materials. *Progress in Polymer Science* **39**, 1–42 (2014).
16. Nightingale, E. R. Phenomenological theory of ion solvation. effective radii of hydrated ions. *The Journal of Physical Chemistry* **63**, 1381–1387 (1959).
17. Bonner, O. D. & Payne, W. H. Equilibrium studies of some monovalent ions on Dowex 50. *The Journal of Physical Chemistry* **58**, 183–185 (1954).
18. Mitroy, J., Safronova, M. S. & Clark, C. W. Theory and applications of atomic and ionic polarizabilities. *Journal of Physics B: Atomic, Molecular and Optical Physics* **43**, 202001 (2010).
19. Mahan, G. D. & Subbaswamy, K. R. *Local density theory of polarizability* (Plenum Press, New York, NY, 1990).
20. Jungwirth, P., Curtis, J. E. & Tobias, D. J. Polarizability and aqueous solvation of the sulfate dianion. *Chemical Physics Letters* **367**, 704–710 (2003).
21. Strathmann, H. *Ion-exchange membrane separation processes* First. *Membrane science and technology series* **9** (Elsevier, Amsterdam ; Boston, 2004).

Chapter 4 |

Conclusions and future work

Understanding the behavior of ions in charged membranes, and how the membrane structure influences the movement of those ions is important for improving performance in applications including desalination, electro dialysis, fuel cells, energy recovery, sensors and facilitated gas transport. This thesis has provided an in-depth look into the effect of different ions on the performance of ion exchange membranes, as well as preliminary work on the use of thin-film thin-film composite membrane structures in order to overcome the permselectivity / resistance trade-off.

Water uptake and permselectivity was measured for five SPES cation exchange membranes in six different salt solutions in order to isolate the specific effect of both counter-ions and co-ions on membrane permselectivity. Membrane permselectivity correlated with both the co-ion and counter-ion used. For counter-ions, the membrane permselectivity ranked Li^+ , Na^+ , K^+ , from high permselectivity to low, while for counter-ions membrane permselectivity ranked Cl^- , SO_4^{2-} , from high permselectivity to low.

Water uptake and fixed charge density were not found to describe permselectivity effects for different salts, meaning specific interactions between the ions and the polymer govern membrane performance for ion exchange membranes.

Strong interactions between counter-ion and fixed charge group (binding affinity) were found to result in counter-ion condensation, leading to lower membrane permselectivity. The ability of the fixed ion group to influence the charge density of the co-ion was found to influence permselectivity, with more polarizable co-ions providing lower membrane permselectivities. Interaction effects between the co-ion and counter-ion were not able to be determined, however future studies will investigate this possibility further.

These tools will allow for the creation of a new class of ion exchange membranes that are specifically tailored to a given application. This will not only allow for improvements in existing technologies, but will allow a host of new technologies to become economically viable with increased efficiencies.

4.1 Future work

4.1.1 Specific ion effects on permselectivity

While the work in this thesis forms a foundation for describing the effects of specific ions on the permselectivity of cation exchange membranes, more ions need to be investigated. This can be subdivided into two tasks; understanding the effect of co-ions on permselectivity, and the effect of counter-ions on permselectivity.

Co-ion effects

The findings of this thesis suggest that co-ion polarizability is a primary factor for describing co-ion permselectivity effects. In order to isolate co-ion effects, it is recommended that the permselectivity of a sulfonated poly(ether sulfone) membrane is measured for different sodium salts. Five anions, summarized in Table 4.1 have been identified as strong candidates for future studies. These ions

Table 4.1: Property data for ions that are recommended for future membrane permselectivity testing.

Ion*	Hydrated radii [Å] ^[1]	Charge density [e ⁻ /nm ³] [†]	Mobility × 10 ⁴ [cm ² /SV] ^[2,3]	Polarizability [au] ^[4-6]	Binding affinity ^[7,8]
Li ⁺	3.82	4.28	4.01	0.19	1.00
Na ⁺	3.58	5.20	5.19	1.00	1.98
K ⁺	3.31	6.58	7.62	5.40	2.90
Mg²⁺	4.28	6.09	5.50	0.49	3.29
Ca²⁺	4.12	6.83	6.17	3.26	5.16
Sr²⁺	4.12	6.83	6.16	5.81	6.51
Ba²⁺	4.04	7.24	6.60	10.5	11.5
Cl ⁻	3.32	6.52	7.91	22.3	
Br ⁻	3.30	6.64	8.13	29.7	
NO ₃ ⁻	3.35	6.35	7.40	30.4 [‡]	
I ⁻	3.31	6.58	7.96	43.2	
SO ₃ ²⁻	3.00	17.7	8.29	35.8 [‡]	
SO ₄ ²⁻	3.79	8.77	8.27	47.2 [‡]	
S₂O₃²⁻				60.0 [‡]	

* Bold items represent new ions recommended for testing, while standard items represent ions tested in this thesis.

† Calculated from the hydrated radii.

‡ These items were computed with a simple model and should be treated as rough approximations.^[6]

were selected because they span a wide range of polarizability, are water soluble in their sodium form and are relatively safe to use.

Chloride, bromide and iodide were selected since polarizability is most reliably calculated for monatomic ions.^[5,9] These three ions are of the same valency and have roughly the same hydrated radius, mobility and charge density, making polarizability is the main differentiating factor. Therefore, these three ions will provide a foundation for looking at of co-ion-polarizability effects in ion exchange membranes. The conclusions of this thesis predicts that higher co-ion polarizability will results in lower permselectivity such that $\Psi_{\text{NaCl}} > \Psi_{\text{NaBr}} > \Psi_{\text{NaI}}$.

The polarizability values for polyatomic ions are not as well-described as

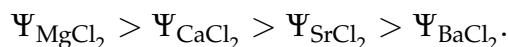
monatomic ions due to the increased complexity of these ions.^[9-11] Many polyatomic ions will speciate upon aqueous solvation leading to multi-ionic solutions. Not only do the tools for evaluating the permselectivity of multi-ionic systems not exist, but even if we could, the presence of other ions would make it impossible to isolate individual ion effects. However, nearly all usable divalent anions are polyatomic, so necessity dictates their use.

Nitrate, sulfite, sulfate and thiosulfate have been selected as polyatomic co-ions recommended for testing. These ions have relatively low levels of speciation, and the three divalent anions will provide insight into co-ion valency effects. Sulfite is of particular interest since it has a similar polarizability and hydrated radius to iodide. The monovalent polyatomic ion nitrate was included because it is of particular interest in the mining and agricultural industry, and gives a monatomic/polyatomic comparison for monovalent anions.

Counter-ion effects

The findings of this thesis suggest that the counter-ion binding affinity to the fixed ion group, and resulting counter-ion condensation are the primary parameter for describing counter-ion permselectivity effects. In order to isolate counter-ion effects, it is recommended that the permselectivity of a sulfonated poly(ether sulfone) membrane is measured for different chloride salts. Four cations, summarized in Table 4.1, have been identified as strong candidates for future studies.

Divalent cations were chosen, because they have a large variation in sulfonate binding affinities. The conclusions of this thesis predict that counter-ions with higher sulfonate binding affinities will have lower permselectivities such that



Barium in particular has an exceedingly high sulfonate binding affinity. Barium sulfate is very insoluble in water with a solubility of $1 \times 10^{-5} \text{ g}_{\text{solute}}/\text{g}_{\text{solution}}$.^[12] Counter-ion condensation might be so large in barium salts that it permanently deactivates the polymer. If polymer swelling is maintained under this condition, no difference should be seen between the ion exchange membrane and a non-selective membrane. It is also possible that the polymer will de-swell under this extreme case, which could maintain selectivity at the expense of high ionic resistance.

Anion exchange membranes

This thesis focuses on sulfonated poly(ether sulfone) cation exchange membranes. While anion exchange membranes and cation exchange membranes are in many ways analogous, they are not identical; the properties used to describe ion transport in cation exchange membranes might not accurately describe transport in anion exchange membranes.

To examine the differences, the study performed in this thesis should be extended to a set of anion exchange membranes. A suitable anion exchange polymer would need to be identified, as well as a set of ions that will represent a similar set of properties to the ions used in this thesis.

4.1.2 Polymer property effects on permselectivity

Properties such as cross-linking can modify water swelling and charge density for a given polymer. Other functional groups such as carboxylic or phosphonic acids can replace sulfonic acid to test the effects of the functional group.^[13,14]

The polymer backbone has been shown to affect polymer morphology; it has been shown using small-angle neutron scattering (SANS) that aPPO will

nanophase at certain levels of functionalization.^[15] Local variations in fixed charge concentration due to nanophase separation could modify ion specific effects. SANS should be performed on sulfonated polymers with different backbones such as sulfonated poly(2,6-dimethyl-1,4-phenylene oxide) (SPPO) and sulfonated poly(ether ether ketone) (SPEEK) to investigate the affect of polymer structure on ion specific effects and permselectivity.

References

1. Nightingale, E. R. Phenomenological theory of ion solvation. effective radii of hydrated ions. *The Journal of Physical Chemistry* **63**, 1381–1387 (1959).
2. Bard, A. J. & Faulkner, L. R. *Electrochemical methods: fundamentals and applications* Second (John Wiley & Sons, Inc., New York, NY, 2001).
3. *Methods of soil analysis part 4: Physical methods* (eds Dane, J. H. & Topp, G. C.) *Soil Science Society of America book series* **5,4** (Soil Science Society of America, Madison, WI, 2002).
4. Mitroy, J., Safronova, M. S. & Clark, C. W. Theory and applications of atomic and ionic polarizabilities. *Journal of Physics B: Atomic, Molecular and Optical Physics* **43**, 202001 (2010).
5. Mahan, G. D. & Subbaswamy, K. R. *Local density theory of polarizability* (Plenum Press, New York, NY, 1990).
6. ChemAxon. *chemicalize* url: <http://www.chemicalize.org/> (2015).
7. Bonner, O. D. & Payne, W. H. Equilibrium studies of some monovalent ions on Dowex 50. *The Journal of Physical Chemistry* **58**, 183–185 (1954).
8. Bonner, O. D. & Smith, L. L. A selectivity scale for some divalent cations on Dowex 50. *The Journal of Physical Chemistry* **61**, 326–329 (1957).
9. Eklund, L., Hofer, T. S., Pribil, A. B., Rode, B. M. & Persson, I. On the structure and dynamics of the hydrated sulfite ion in aqueous solution - an ab initio QMCF MD simulation and large angle X-ray scattering study. *Dalton Transactions* **41**, 5209 (2012).
10. Lucy, C. A. Factors affecting selectivity of inorganic anions in capillary electrophoresis. *Journal of Chromatography A* **850**, 319–337 (1999).
11. Jungwirth, P., Curtis, J. E. & Tobias, D. J. Polarizability and aqueous solvation of the sulfate dianion. *Chemical Physics Letters* **367**, 704–710 (2003).
12. Haynes, W. M. *CRC handbook of chemistry and physics: a ready-reference book of chemical and physical data* (2014).
13. Van der Bruggen, B. Chemical modification of polyethersulfone nanofiltration membranes: A review. *Journal of Applied Polymer Science* **114**, 630–642 (2009).

14. Botvay, A., Máthé, Á. & Pöpl, L. Nitration of polyethersulfone by ammonium nitrate and trifluoroacetic anhydride. *Polymer* **40**, 4965–4970 (1999).
15. Geise, G. M., Hickner, M. A. & Logan, B. E. Ammonium bicarbonate transport in anion exchange membranes for salinity gradient energy. *ACS Macro Letters* **2**, 814–817 (2013).